1 The Morphology of the Electrocardiogram

Antoni Bayés de Luna, Velislav N. Batchvarov and Marek Malik

Summary

The 12-lead electrocardiogram (ECG) is the single most commonly performed investigation. Almost every hospitalized patient will undergo electrocardiography, and patients with known cardiovascular disease will do so many times. In addition, innumerable ECGs recorded are made for life insurance, occupational fitness and routine purposes. Most ECG machines are now able to read the tracing; many of the reports are accurate but some are not. However, an accurate interpretation of the ECG requires not only the trace but also clinical details relating to the patient. Thus, every cardiologist and physician/cardiologist should be able to understand and interpret the 12-lead ECG. Nowadays, many other groups, for example accident and emergency physicians, anaesthetists, junior medical staff, coronary care, cardiac service and chest pain nurses, also need a good grounding in this skill. In the last several decades a variety of new electrocardiographic techniques, such as short- and long-term ambulatory ECG monitoring using wearable or implantable devices, event ECG monitoring, single averaged ECGs in the time, frequency and spatial domains and a variety of stress recoding methods, have been devised. The cardiologist, at least, must understand the application and value of these important clinical investigations. This chapter deals comprehensively with 12-lead electrocardiography and the major pathophysiological conditions that can be revealed using this technique. Cardiac arrhythmias and other information from ambulatory and averaging techniques are explained only briefly but are more fully covered in other chapters, for example those devoted to specific cardiac arrhythmias.

Introduction

Broadly speaking, electrocardiography, i.e. the science and practice of making and interpreting recordings of cardiac electrical activity, can be divided into morphology and arrhythmology. While electrocardiographic morphology deals with interpretation of the shape (amplitude, width and contour) of the electrocardiographic signals, arrhythmology is devoted to the study of the rhythm (sequence and frequency) of the heart. Although these two parts of electrocardiography are closely interlinked, their methodological distinction is appropriate. Intentionally, this chapter covers only electrocardiographic morphology since rhythm abnormalities are dealt with elsewhere in this book.

Morphology of the ECG

The electrocardiogram (ECG), introduced into clinical practice more than 100 years ago by Einthoven, comprises a linear recording of cardiac electrical activity as it occurs over time. An atrial depolarization wave (P wave), a ventricular depolarization wave (QRS complex) and a ventricular repolarization wave (T wave) are successively

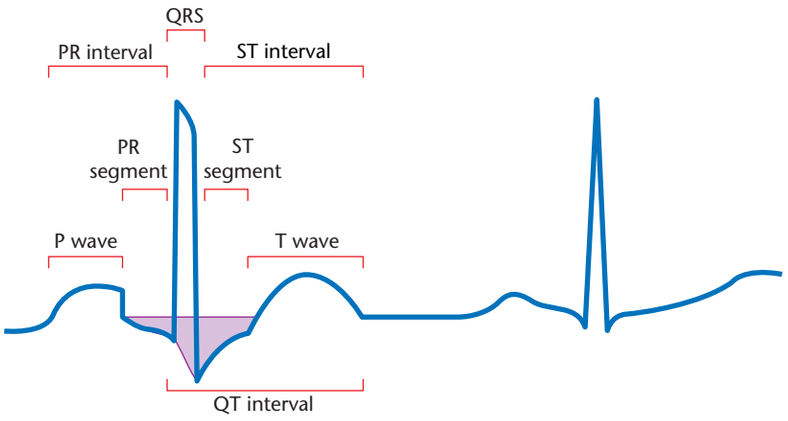

Figure 1.1 ECG morphology recorded in a lead facing the left ventricular free wall showing the different waves and intervals. Shading, atrial repolarization wave.

recorded for each cardiac cycle (Fig. 1.1). During normal sinus rhythm the sequence is always P–QRS–T. Depending on heart rate and rhythm, the interval between waves of one cycle and another is variable.

Electrophysiological principles [1–6]

The origin of ECG morphology may be explained by the dipole-vector theory, which states that the ECG is an expression of the electro-ionic changes generated during myocardial depolarization and repolarization. A pair of electrical charges, termed a dipole, is formed during both depolarization and repolarization processes (Fig. 1.2). These dipoles have a vectorial expression, with the head of the vector located at the positive pole of a dipole. An electrode that faces the head of the vector records a positive deflection.

To ascertain the direction of a wavefront, the ECG is recorded from different sites, termed 'leads'. When recording the 12-lead ECG six frontal leads (I, II, III, aVR, aVL, aVF) and six horizontal leads (V1–V6) are used. There are three bipolar leads in the frontal plane that connect the left to right arm (I), the left leg to right arm (II) and the left leg to left arm (III). According to Einthoven's law, the voltage in each lead should fit the equation II = I + III. These three leads form Einthoven's triangle (Fig. 1.3A). Bailey obtained a reference figure (Bailey's triaxial system) by shifting the three leads towards the centre.

There are also three augmented bipolar leads (aVR, aVL and aVF) in the frontal plane (Fig. 1.3B). These are de-

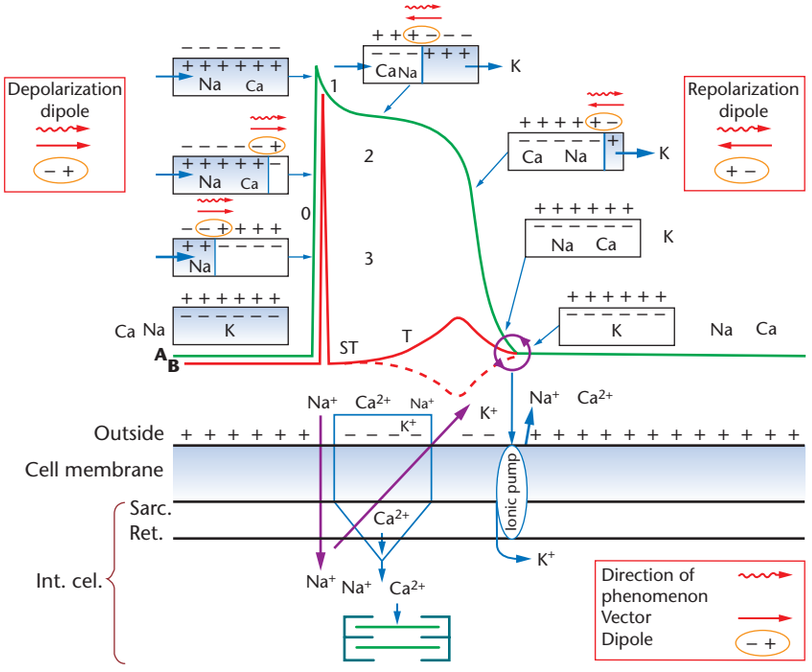

Figure 1.2 Scheme of electro-ionic changes that occur in the cellular depolarization and repolarization in the contractile myocardium. (A) Curve of action potential. (B) Curve of the electrogram of a single cell (repolarization with a dotted line) or left ventricle (normal curve of ECG with a positive continuous line). In phase 0 of action potential coinciding with the Na^+ entrance, the depolarization dipole (–+) and, in phase 2 with the K^+ exit, the repolarization dipole (+–), are originated. At the end of phase 3 of the action potential an electrical but not ionic balance is obtained. For ionic balance an active mechanism (ionic pump) is necessary.

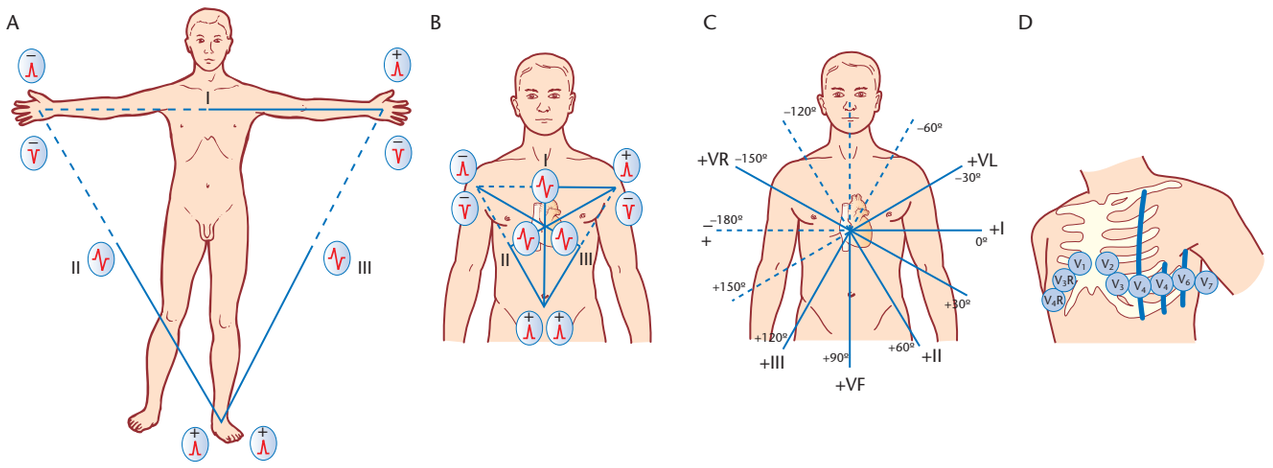

Figure 1.3 (A) Einthoven's triangle. (B) Einthoven's triangle superimposed on a human thorax. Note the positive (continuous line) and negative (dotted line) part of each lead. (C) Bailey's hexaxial system. (D) Sites where positive poles of the six precordial leads are located.

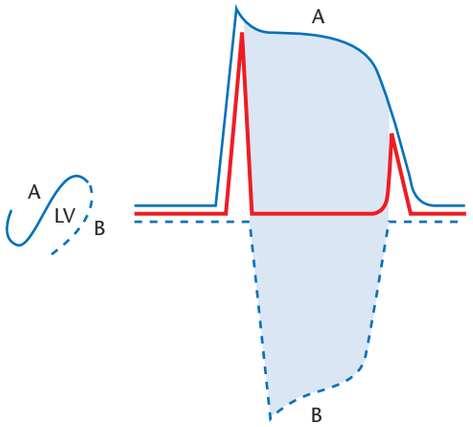

Figure 1.4 Correlation between global action potential, i.e. the sum of all relevant action potentials, of the subendocardial (A) and subepicardial (B) parts of the left ventricle and the ECG waveform. Depolarization starts first in the furthest zone (subendocardium) and repolarization ends last in the furthest zone (subendocardium). When the global action potential of the nearest zone is 'subtracted' from that of the furthest zone, the ECG pattern results. (LV = left ventricle.)

scribed as 'augmented' because, according to Einthoven's law, their voltage is higher than that of the simple bipolar leads. By adding these three leads to Bailey's triaxial system, Bailey's hexaxial system is obtained (Fig. 1.3C). In the horizontal plane, there are six unipolar leads (V1–V6) (Fig. 1.3D).

One approach to understanding ECG morphology is based on the concept that the action potential of a cell or the left ventricle (considered as a huge cell that contributes to the human ECG) is equal to the sum of subendocardial and subepicardial action potentials. How this occurs is shown in Fig. 1.4. This concept is useful for understanding how the ECG patterns of ischaemia and injury are generated (see Fig. 1.17).

Normal characteristics

Heart rate

Normal sinus rhythm at rest is usually said to range from 60 to 100 b.p.m. but the nocturnal sleeping heart rate may fall to about 50 b.p.m. and the normal daytime resting heart rate rarely exceeds 90 b.p.m. Several methods exist to assess heart rate from the ECG. With the standard recording speed of 25 mm/s, the most common method is to divide 300 by the number of 5-mm spaces (the graph paper is divided into 1- and 5-mm squares) between two consecutive R waves (two spaces represents 150 b.p.m., three spaces 100 b.p.m., four spaces 75 b.p.m., five spaces 60 b.p.m., etc.).

Rhythm

The cardiac rhythm can be normal sinus rhythm (emanating from the sinus node) or an ectopic rhythm (from a site other than the sinus node). Sinus rhythm is considered to be present when the P wave is positive in I, II, aVF and V2–V6, positive or biphasic (+/–) in III and V1, positive or –/+ in aVL, and negative in aVR.

PR interval and segment

The PR interval is the distance from the beginning of the P wave to the beginning of the QRS complex (Fig. 1.1). The normal PR interval in adult individuals ranges from

0.12 to 0.2 s (up to 0.22 s in the elderly and as short as 0.1 s in the newborn). Longer PR intervals are seen in cases of atrioventricular (AV) block and shorter PR intervals in pre-excitation syndromes and various arrhythmias. The PR segment is the distance from the end of the P wave to QRS onset and is usually isoelectric. Sympathetic overdrive may explain the down-sloping PR segment that forms part of an arc with the ascending nature of the ST segment. In pericarditis and other diseases affecting the atrial myocardium, as in atrial infarction, a displaced and sloping PR segment may be seen.

QT interval

The QT interval represents the sum of depolarization (QRS complex) and repolarization (ST segment and T wave) (Fig. 1.1). Very often, particularly in cases of a flat T wave or in the presence of a U wave, it is difficult to measure the QT interval accurately. It is usual to perform this measurement using a consistent method in order to ensure accuracy if the QT interval is studied sequentially. The recommended method is to consider the end of repolarization as the point where a tangent drawn along the descending slope of the T wave crosses the isoelectric line. The best result may be obtained by measuring the median duration of QT simultaneously in 12 leads. Automatic measurement may not be accurate but is often used clinically [7].

It is necessary to correct the QT interval for heart rate (QTc). Different heart rate correction formulae exist. The most frequently used are those of Bazett and Fridericia:

$$\text{Bazett (square root) correction: QT corrected} = \text{QT measured}/\text{RR interval (s)}^{0.5}$$

$$\text{Fridericia (cube root) correction: QT corrected} = \text{QT measured}/\text{RR interval (s)}^{0.33}$$

Although these correction methods are not accurate and are highly problematic in cases when a very precise QTc value is needed, their results are satisfactory in standard clinical practice. Because of its better accuracy the Fridericia formula is preferred to that of Bazett.

A long QT interval may occur in the congenital long QT syndromes or can be associated with sudden death [8], heart failure, ischaemic heart disease, bradycardia, some electrolyte disorders (e.g. hypokalaemia and hypocalcaemia) and following the intake of different drugs. Generally, it is believed that if a drug increases the QTc by more than 60 ms, torsade de pointes and sudden cardiac death might result. However, torsade de pointes rarely occurs unless the QTc exceeds 500 ms [9]. A short QT interval can be found in cases of early repolarization, in association with digitalis and, rarely, in a genetic disorder associated with sudden death [10].

P wave

This is the atrial depolarization wave (Fig. 1.1). In general, its height should not exceed 2.5 mm and its width should not be greater than 0.1 s. It is rounded and positive but may be biphasic in V1 and III and –/+ in aVL. The atrial repolarization wave is of low amplitude and usually masked by coincident ventricular depolarization (QRS complex) (see shading in Fig. 1.1).

QRS complex

This results from ventricular depolarization (Figs 1.1 and 1.5). According to Durrer *et al*. [11], ventricular depolarization begins in three different sites in the left ventricle and occurs in three consecutive phases that give rise to the generation of three vectors [6].

The ventricular depolarization signal is often described generically as a QRS complex. Usually the deflection is triphasic and, provided that the initial wave is negative (down-going), the three waves are sequentially known as Q, R and S. If the first part of the complex is up-going the deflection is codified as an R wave, etc. If the R or S wave is large in amplitude, upper case letters (R, S) are used, but if small in amplitude, lower case letters (r, s) are used. A normal or physiological initial negative wave of the ventricular depolarization waveform is called a q wave. It must be narrow (< 0.04 s) and should not usually exceed 25% of the amplitude of the following R wave, though some exceptions exist mainly in leads III, aVL and aVF. If the initial deflection is wider or deeper, it is known as a Q wave. Different morphologies are presented in Fig. 1.5.

The QRS width should not exceed 0.095 s and the R wave height should not exceed 25 mm in leads V5 and V6 or 20 mm in leads I and aVL, although a height greater than 15 mm in aVL is usually abnormal.

ST segment and T wave

The T wave, together with the preceding ST segment, is formed during ventricular repolarization (Fig. 1.1). The T wave is generally positive in all leads except aVR, but may be negative, flattened or only slightly positive in V1, and flattened or slightly negative in V2, III and aVF. The T wave presents an ascending slope with slower inscription than the descending slope. In children, a negative T wave is normal when seen in the right precordial leads (paediatric repolarization pattern) (Fig. 1.6F). Under normal conditions, the ST segment is isoelectric or shows only a slight down-slope (< 0.5 mm). Examples of normal ST–T wave variants are displayed in Fig. 1.6 (the figure caption provides comment on these patterns). Occasion-

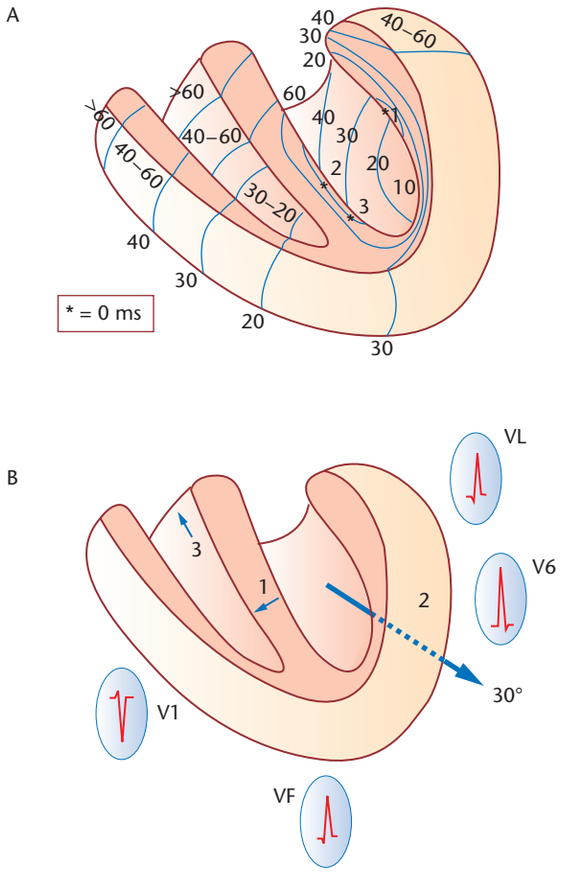

Figure 1.5 (A) The three initial points (1, 2, 3) of ventricular depolarization are marked by asterisks. The isochrone lines of the depolarization sequence can also be seen (time shown in ms). (B) The first vector corresponds to the sum of depolarization of the three points indicated in (A) and because it is more potent than the forces of the right vector, the global direction of vector 1 will be from left to right. The second vector corresponds to depolarization of the majority of the left ventricle and usually is directed to the left, downward and backward. The third vector represents the depolarization of basal parts of the septum and right ventricle.

ally, after a T wave, a small U wave can be observed, usually showing the same polarity as the T wave (Fig. 1.1).

Electrocardiographic morphological abnormalities

Electrocardiography can be considered the test of choice or the gold standard for the diagnosis of AV blocks, abnormal intra-atrial and intraventricular conduction, ventricular pre-excitation, most cardiac arrhythmias and, to some extent, acute myocardial infarction. However, in other cases, such as atrial and ventricular enlargement, abnormalities secondary to chronic coronary artery disease (ECG pattern of ischaemia, injury or necrosis), other repolarization abnormalities and certain arrhythmias, electrocardiography provides useful information and may suggest the diagnosis based on predetermined electrocardiographic criteria. However, these criteria have lesser diagnostic potential compared with other electrocardiology or imaging techniques (e.g. echocardiography in atrial or ventricular enlargement). In some circumstances, electrocardiography is the technique of choice and the electrocardiographic criteria in use are diagnostic for those conditions (e.g. bundle branch block), while for other conditions (e.g. cavity enlargement) the criteria are only indicative. In order to know the real value of the ECG criteria in these cases, it is important to understand the concepts of sensitivity, specificity and predictive accuracy [1].

Atrial abnormalities

Electrocardiographic patterns observed in patients with atrial hypertrophy and atrial dilation (atrial enlargement) and with atrial conduction block are encompassed by this term (Fig. 1.7).

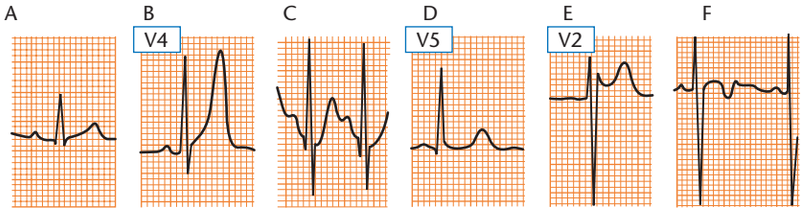

Figure 1.6 Different morphologies of normal variants of the ST segment and T wave in the absence of heart disease. (A) Normal ST/T wave. (B) Vagotonia and early repolarization. (C) Sympathetic overdrive. ECG of a 22-year-old male obtained with continuous Holter monitoring during a parachute jump. (D) Straightening of ST with symmetric T wave in a healthy 75-year-old man without heart disease. (E) Normal variant of ST ascent (saddle morphology) in a 20-year-old man with pectus excavatum. (F) Normal repolarization in a 3-year-old child.

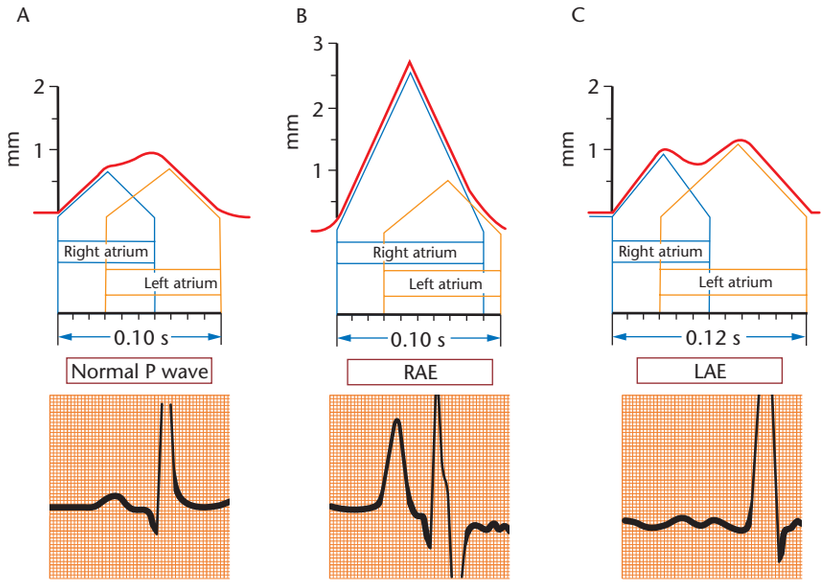

Figure 1.7 Schematic diagrams of atrial depolarization in (A) normal P wave, (B) right atrial enlargement (RAE) and (C) left atrial enlargement (LAE) with interatrial conduction block. An example of each of these P waves is shown beneath each diagram.

Right atrial enlargement (Fig. 1.7B)

Right atrial enlargement is usually present in patients with congenital and valvular heart diseases affecting the right side of the heart and in cor pulmonale.

Diagnostic criteria

The diagnostic criteria of right atrial abnormality are based on P-wave amplitude abnormalities (≥ 2.5 mm in II and/or 1.5 mm in V1) and ECG features of associated right ventricular abnormalities.

Left atrial enlargement (Fig. 1.7C)

Left atrial enlargement is seen in patients with mitral and aortic valve disease, ischaemic heart disease, hypertension and some cardiomyopathies.

Diagnostic criteria

1. P wave with duration ≥ 0.12 s especially seen in leads I or II, generally bimodal, but with a normal amplitude.
2. Biphasic P wave in V1 with a terminal negative component of at least 0.04 s. Criteria 1 and 2 have good specificity (close to 90%) but less sensitivity (< 60%).
3. P wave with biphasic (±) morphology in II, III and aVF with duration ≥ 0.12 s, which is very specific (100% in valvular heart disease and cardiomyopathies) but has low sensitivity for left atrial abnormality [12,13].

Interatrial block

PARTIAL BLOCK

P-wave morphology is very similar to that seen with left atrial abnormality. Usually the negative part in V1 may be less prominent than in atrial hypertrophy or dilation, although it is not surprising that the morphology of left atrial abnormality and atrial block are similar because the features of left atrial abnormality are more dependent on delayed interatrial conduction than on atrial dilation.

ADVANCED INTERATRIAL BLOCK WITH LEFT ATRIAL RETROGRADE ACTIVATION

This is characterized by a P wave with duration ≥ 0.12 s and with biphasic (±) morphology in II, III and aVF. A biphasic P-wave morphology in V1 to V3/V4 is also frequent (see below). This morphology is a marker for paroxysmal supra-ventricular tachyarrhythmias [12,13] and is very specific (100%) for left atrial enlargement.

Ventricular enlargement

The electrocardiographic concept of enlargement of the right and left ventricle encompasses both hypertrophy and dilation and, of course, the combination. The diagnostic criteria for ventricular enlargement when QRS duration is less than 120 ms are set out below. The criteria for the diagnosis of right and/or left ventricular enlargement combined with intraventricular block (QRS duration ≥ 120 ms) are defined elsewhere [1,5,14,15].

Right ventricular enlargement

Right ventricular enlargement (RVE) is found particularly in cases of congenital heart disease, valvular heart disease and cor pulmonale. Figure 1.8 shows that

Table 1.1 Electrocardiographic criteria of right ventricular enlargement

	Criterion	Sensitivity (%)	Specificity (%)
V1	R/S V1 ≥ 1	6	98
	R V1 ≥ 7 mm	2	99
	qR in V1	5	99
	S in V1 < 2 mm	6	98
	IDT in V1 ≥ 0.35 s	8	98
V5-V6	R/S V5–V6 ≤ 1	16	93
	R V5–V6 < 5 mm	13	87
	S V5–V6 ≥ 7 mm	26	90
V1 + V6	RV1 + SV5-V6 > 10.5 mm	18	94
ÂQRS	ÂQRS ≥ 110°	15	96
	SI, SII, SIII	24	87

IDT, intrinsicoid deflection (time from QRS onset to R wave peak).

Table 1.2 Morphologies with dominant R or R′ (r′) in V1

Clinical setting	QRS width	P-wave morphology in V1
No heart disease		
Incorrect electrode placement	< 0.12 s	Various changes
Normal variant (post-term infants, scant Purkinje fibres in anteroseptal zone)	< 0.12 s	Normal
Chest anomalies	< 0.12 s	Normal
Typical right bundle branch block	From < 0.12 to ≥ 0.12 s	Normal
Atypical right bundle branch block		
Ebstein's disease	Often ≥ 0.12 s	Often tall, peaked and + or ±
Arrhythmogenic right ventricular dysplasia	Often ≥ 0.12 s	Often abnormal
Brugada's syndrome	Sometimes ≥ 0.12 s	Normal
Right ventricular or biventricular enlargement (hypertrophy)	< 0.12 s	Often tall and peaked
Wolff–Parkinson–White syndrome	From < 0.12 to ≥ 0.12 s	Normal P, short PR
Lateral myocardial infarction	< 0.12 s	Normal P

the ECG pattern in V1 (prominent R wave) is related more to the degree of RVE than to its aetiology.

Diagnostic criteria

The electrocardiographic criteria most frequently used for the diagnosis of RVE are shown in Table 1.1, along with their sensitivities (low) and specificities (high). The differential diagnosis of an exclusive or dominant R wave in V1 (R, Rs or rSR′ pattern) is given in Table 1.2.

1 Morphology in V1: morphologies with a dominant or exclusive R wave in V1 are very specific, but not so sensitive (< 10%) for the diagnosis of RVE. Nevertheless, other causes that may cause a dominant R pattern in V1 must be excluded (see Table 1.2). An rS or even QS morphology in V1, together with RS in V6, may often be observed in chronic cor pulmonale, even in advanced stages or in the early stages of RVE of other aetiologies (Fig. 1.8).

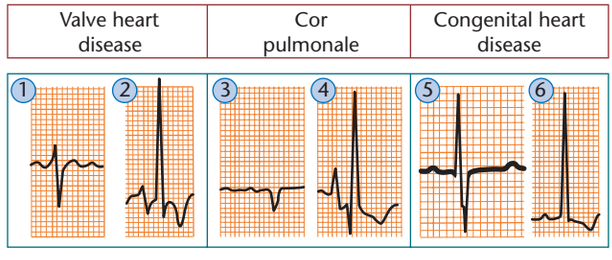

Figure 1.8 ECG pattern of right ventricular enlargement: note that QRS in V1 depends more on the severity of right ventricular enlargement than on aetiology of the disease. 1, 3 and 5 represent examples of mild mitral stenosis, cor pulmonale and congenital pulmonary stenosis respectively, while 2, 4 and 6 are cases of severe and long-standing mitral stenosis, cor pulmonale with severe pulmonary hypertension, and congenital pulmonary stenosis respectively.

2 Morphology in V6: the presence of forces directed to the right expressed as an S wave in V5–V6 is one of the most important ECG criteria.
3 Frontal plane QRS electrical axis (ÂQRS): ÂQRS ≥ 110° is a criterion with low sensitivity but high specificity (95%) provided that left posterior hemiblock, an extremely vertical heart position and lateral left ventricular wall infarction have been excluded.
4 SI, SII, SIII: an S wave in the three bipolar limb leads is frequently seen in chronic cor pulmonale with a QS or rS pattern in V1 and an RS pattern in V6. The possibility of this pattern being secondary to a positional change or simply to peripheral right ventricular block must be excluded [16].

The combination of more than one of these criteria increases the diagnostic likelihood. Horan and Flowers [15] have published a scoring system based on the most frequently used ECG criteria for right ventricular enlargement.

Left ventricular enlargement

Left ventricular enlargement, or ischaemic heart disease, is found particularly in hypertension, valvular heart disease, cardiomyopathies and in some congenital heart diseases.

In general, in patients with left ventricular enlargement, the QRS voltage is increased and is directed more posteriorly than normal. This explains why negative QRS complexes predominate in the right precordial leads. Occasionally, probably related to significant cardiac laevorotation or with more significant hypertrophy of the left ventricular septal area than of the left ventricular free wall, as occurs in some cases of apical hypertrophic cardiomyopathy, the maximum QRS is not directed posteriorly. In this situation a tall R wave may be seen even in V2.

The normal q wave in V6 may not persist if hypertrophy is associated with fibrosis and/or partial left bundle branch block. In Fig. 1.9, the ECG from a case of aortic valvular disease without septal fibrosis shows a q wave in V6 and a positive T wave, whereas the ECG from another case with fibrosis does not have a q wave in V6 [17,18]. The ECG pattern is more related to disease evolution than to the haemodynamic overload (Fig. 1.10), although a q wave in V5–V6 remains more frequently in long-standing aortic regurgitation than in aortic stenosis. The pattern of left ventricular enlargement is usually fixed but may be partially resolved with medical treatment of hypertension or surgery for aortic valvular disease.

Diagnostic criteria

Various diagnostic criteria exist (Table 1.3). Those with good specificity (≥ 95%) and acceptable sensitivity (40–50%) include the Cornell voltage criteria and the Romhilt and Estes scoring system.

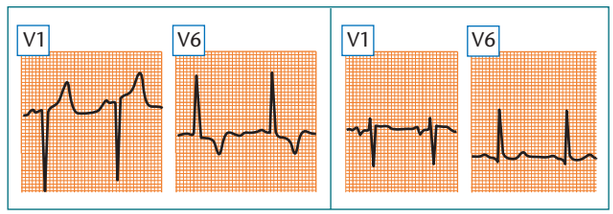

Figure 1.9 The most characteristic ECG feature of left ventricular enlargement is tall R waves in V5–6 and deep S waves in V1–2. The presence of a normal septal q wave depends on whether septal fibrosis is present. This figure shows two examples of aortic valvular disease both with left ventricular enlargement: (A) no fibrosis and a normal septal q wave; (B) abnormal ECG (ST/T with strain pattern) and no septal q wave due to extensive fibrosis.

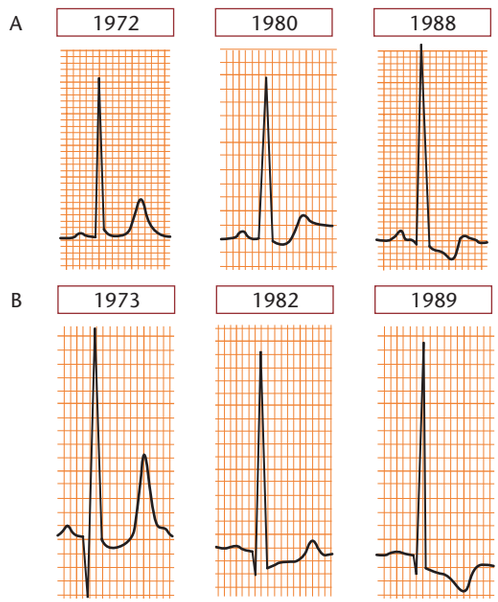

Figure 1.10 Examples of different ECG morphologies seen during the evolution of aortic stenosis (A) and aortic regurgitation (B).

Intraventricular conduction blocks

Ventricular conduction disturbances or blocks can occur on the right side or on the left. They can affect an entire ventricle or only part of it (divisional block). The block of conduction may be first degree (partial block or conduction delay) when the stimulus conducts but with

Table 1.3 Electrocardiographic criteria of left ventricular enlargement

Voltage criteria	Sensitivity (%)	Specificity (%)
RI + SIII > 25 mm	10.6	100
R aVL > 11 mm	11	100
R aVL > 7.5 mm	22	96
SV1 + RV5–6 ≥ 35 mm (Sokolow–Lyon)	22	100
RV5–6 > 26 mm	25	98
Cornell voltage criterion: R aVL + SV3 > 28 mm (men) or 20 mm (women)	42	96
Cornell voltage duration: QRS duration × Cornell voltage > 2436 mm/seg	51	95
In V1–V6, deepest S + tallest R > 45 mm	45	93
Rohmilt–Estes score > 4 points	55	85
Rohmilt–Estes score > 5 points	35	95

delay, third degree (advanced block) when passage of the wavefront is completely blocked, and second degree when the stimulus sometimes passes and sometimes does not.

Advanced or third-degree right bundle branch block (Fig. 1.11)

Advanced right bundle branch block (RBBB) represents complete block of stimulus in the right bundle or within the right ventricular Purkinje network. In this situation, activation of the right ventricle is initiated by condution through the septum from the left-sided Purkinje system.

Diagnostic criteria

1. QRS ≥ 0.12 s with slurring in the mid-final portion of the QRS.
2. V1: rsR′ pattern with a slurred R wave and a negative T wave.
3. V6: qRs pattern with S-wave slurring and a positive T wave.
4. aVR: QR with evident R-wave slurring and a negative T wave.
5. T wave with polarity opposite to that of the slurred component of the QRS.

Partial or first-degree RBBB

In this case, activation delay of the ventricle is less delayed. The QRS complex is 0.1–0.12 s in duration, but V1 morphology is rsR′ or rsr′.

Advanced (third degree) left bundle branch block (Fig. 1.12)

Advanced left bundle branch block (LBBB) represents complete block of stimulus in the left bundle or within the left ventricular Purkinje network. In this situation, activation of the left ventricle is initiated by conduction through the septum from the right-sided Purkinje system.

Diagnostic criteria

1. QRS ≥ 0.12 s, sometimes over 0.16 s, especially with slurring in the mid-portion of the QRS.
2. V1: QS or rS pattern with a small r wave and a positive T wave.
3. I and V6: a single R wave with its peak after the initial 0.06 s (delayed intrinsicoid deflection).
4. aVR: a QS pattern with a positive T wave.
5. T waves with their polarity usually opposite to the slurred component of the QRS complex.

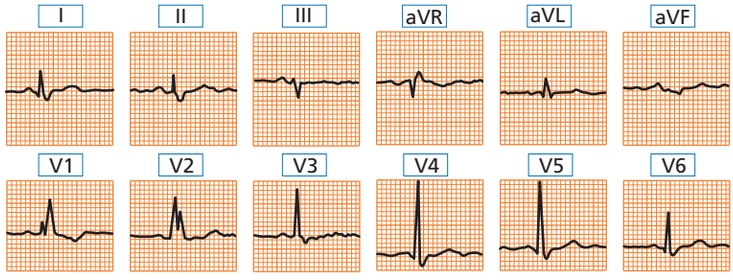

Figure 1.11 ECG in a case of advanced right bundle branch block.

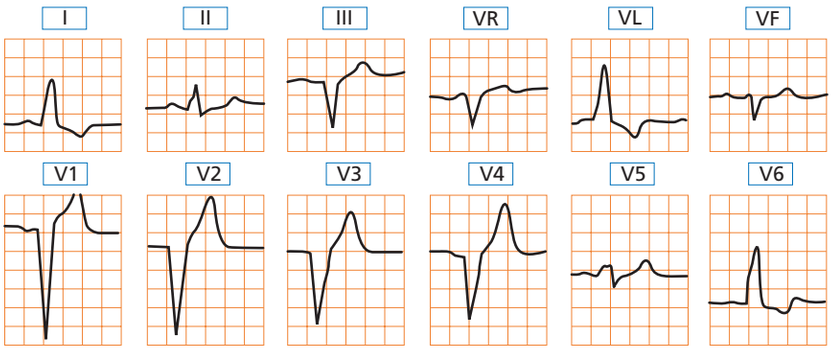

Figure 1.12 ECG in a case of complete left bundle branch block.

Partial or first-degree LBBB

In this case, left ventricular activation is less delayed. The QRS complex is 0.1–0.12 s in duration and presents as a QS complex or a small r wave in V1 and a single R wave in I and V6. This is explained by the fact that due to the delay in activation the first vector that is responsible for formation of the r wave in V1 and the q wave in V6 is not formed. This pattern is partly explained by the presence of septal fibrosis [17].

Divisional left ventricular block (hemiblocks)

The stimulus is blocked or delayed in either the supero-anterior (left anterior hemiblock) or inferoposterior division (left posterior hemiblock) of the left bundle branch [19].

LEFT ANTERIOR HEMIBLOCK

A typical example of left anterior hemiblock (LAH) is illustrated in Fig. 1.13. The differences between LAH and the SI, SII, SIII pattern can also be seen. Inferior wall myocardial infarction and Wolff–Parkinson–White (WPW) syndrome should also be ruled out.

Diagnostic criteria

1 QRS complex duration < 0.12 s.
2 ÂQRS deviated to the left (mainly between –45° and –75°).
3 I and aVL: qR, in advanced cases with slurring especially of the descending part of R wave.
4 II, III and aVF: rS with SIII > SII and RII > RIII.
5 S wave seen up to V6.

LEFT POSTERIOR HEMIBLOCK

In order to make the diagnosis of left posterior hemiblock (LPH), electrocardiographic and clinical characteristics (mainly RVE and an asthenic habitus) must be absent. It is also helpful if evidence of other left ventricular abnormalities is present. A typical electrocardiographic morphology in the frontal and horizontal planes of LPH is shown in Fig. 1.14b.

Diagnostic criteria

1 QRS complex duration < 0.12 s.
2 ÂQRS shifted to the right (between +90° and +140°).
3 I and aVL: RS or rS pattern.
4 II, III and aVF: qR morphology.
5 Precordial leads: S waves up to V6.

The evidence that the ECG pattern suddenly appears confirms the diagnosis of LPH (see Fig. 1.14).

Bifascicular blocks

The two most characteristic bifascicular blocks are advanced RBBB plus LAH and advanced RBBB plus LPH. On some occasions there is RBBB with alternans

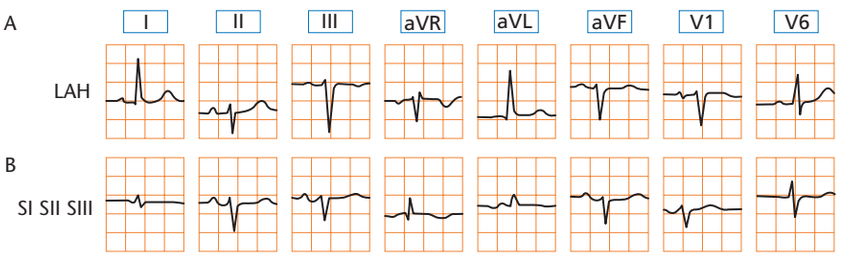

Figure 1.13 (A) An example of left anterior hemiblock. (B) SI SII SIII pattern. See in this case SII > SIII and there is S in lead I.

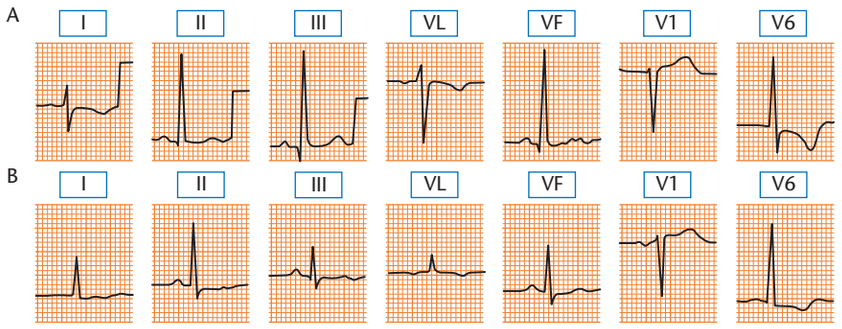

Figure 1.14 (A) An example of left posterior hemiblock. (B) The ECG of same patient some days before. The sudden appeareance of ÂQRS shifted to the right confirms the diagnosis of LPH.

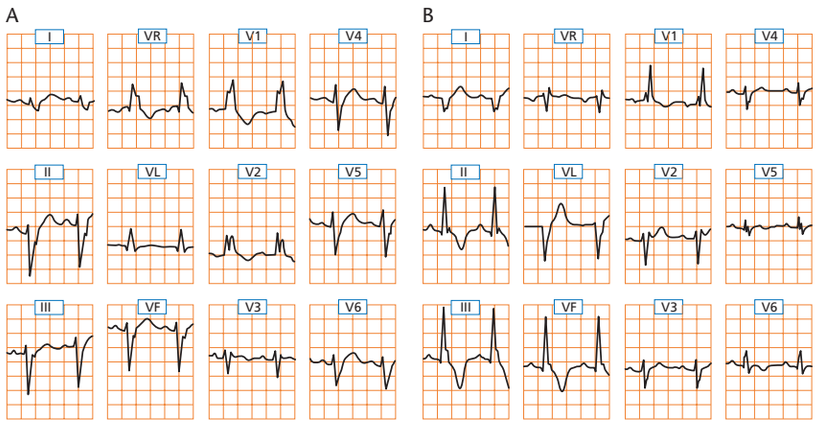

Figure 1.15 (A) Right bundle branch block plus left anterior hemiblock and, the following day, (B) right bundle branch block plus left posterior hemiblock.

of LAH and LPH (one form of trifascicular block) (Fig. 1.15).

ADVANCED RBBB PLUS LAS (Fig. 1.15A)
The diagnostic criteria are as follows.

1 QRS complex duration > 0.12 s.
2 QRS complex morphology: the first portion is directed upwards and to the left as in LAH, while the second portion is directed anteriorly and to the right as in advanced RBBB.

ADVANCED RBBB PLUS LPH (Fig. 1.15B)
The diagnostic criteria are as follows.

1 QRS complex duration > 0.12 s.
2 QRS complex morphology: the first portion of the QRS complex is directed downwards as in isolated LPH, while the second portion is directed anteriorly and to the right similar to advanced RBBB.

Ventricular pre-excitation

Ventricular pre-excitation (early excitation) occurs when the depolarization wavefront reaches the ventricles earlier (via an anomalous pathway) than it would normally (via the AV node/His–Purkinje conduction system). Early excitation is explained by fast conduction through the anomalous pathway that connects the atria with the ventricles, the so-called Kent bundles (WPW-type pre-excitation) [20]. Sometimes, pre-excitation of the His–Purkinje network occurs because of an anomalous atrio-His tract (or simply because of the presence of accelerated AV conduction). This produces short PR-type pre-excitation, called Lown–Ganong–Levine syndrome when associated with junctional tachycardias [21]. Rarely, an anomalous pathway including a section of the normal or accessory AV nodal tissue (Mahaim fibre) produces pre-excitation [22]. The importance of pre-excitation lies in its association with supraventricular tachycardias and sometimes sudden death [23] and the risk of its being mistaken (in the case of WPW pre-excitation) for other pathologies, such as myocardial infarction or hypertrophy. The presence of pre-excitation may also mask other ECG diagnoses.

WPW-type pre-excitation [20,23–25]

The electrocardiographic diagnosis is made by the presence of a short PR interval plus QRS abnormalities characterized by a slurred onset (delta wave) (Fig. 1.16) and T-wave abnormalities.

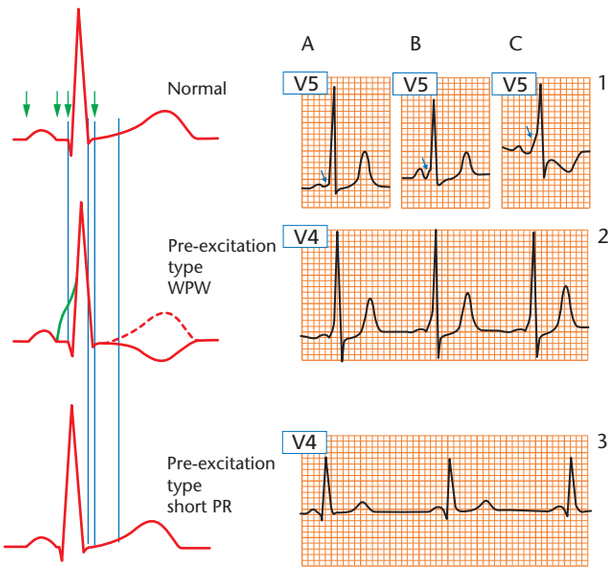

Figure 1.16 *Left*: Comparison of ECGs with normal ventricular activation, Wolff–Parkinson–White (WPW)-type pre-excitation and short PR-type pre-excitation. *Right*: (1) delta waves of different magnitude: (A) minor pre-excitation; (B, C) significant pre-excitation; (2) three consecutive QRS complexes with evident WPW-type pre-excitation; (3) short PR-type pre-excitation.

SHORT PR INTERVAL

In WPW pre-excitation, the PR interval is usually between 0.08 and 0.11 s. However, this form of pre-excitation can also occur with a normal PR interval in the presence of conduction delay within the anomalous pathway or because the anomalous pathway is remotely situated (usually left-sided). Only comparison with a baseline ECG tracing without pre-excitation will confirm whether the PR interval is shorter than usual.

QRS ABNORMALITIES

The QRS complexes are abnormal, i.e. wider than normal (often > 0.11 s) with a characteristic initial slurring (delta wave), caused by early direct activation of the ventricular myocardium as opposed to activation via the His–Purkinje network (Fig. 1.16). Different degrees of pre-excitation (more or less delta wave, QRS widening and T-wave abnormalities; see below) may be observed [1].

QRS complex morphology in the different surface ECG leads depends on the ventricular location of the anomalous pathway. Accordingly, WPW-type pre-excitation may be divided with respect to the location of the pathway [1]. Different algorithms exist to predict the location of the anomalous pathway [25]. However, electrophysiological studies are required to determine the exact location. Precise localization of the anomalous pathway is critical for successful ablation, a procedure performed to destroy the pathway, eliminate pre-excitation and avoid recurrence of paroxysmal supraventricular tachycardias.

REPOLARIZATION ABNORMALITIES

Repolarization is altered (T-wave polarity opposite to that of the pre-excited R wave) except in cases with minor pre-excitation. The changes are secondary to the alteration of depolarization and are more prominent when pre-excitation is greater.

DIFFERENTIAL DIAGNOSIS OF WPW-TYPE PRE-EXCITATION

Right-sided pre-excitation can be mistaken for LBBB; left-sided pre-excitation can be mistaken for RBBB, RVE and various myocardial infarction patterns. In all these cases, a short PR interval and the presence of a delta wave indicate the correct diagnosis of WPW-type pre-excitation.

SPONTANEOUS OR PROVOKED CHANGES IN MORPHOLOGY DUE TO ANOMALOUS CONDUCTION

Changes in the degree of pre-excitation are frequent. Pre-excitation can increase if conduction through the AV node is depressed (vagal manoeuvres, drugs, etc.) and can decrease if AV node conduction is enhanced (adrenaline, physical exercise, etc.).

Short PR-type pre-excitation (Lown–Ganong–Levine syndrome)

This type of pre-excitation is characterized by a short PR interval without changes in QRS morphology [21] (Fig. 1.16). It is impossible to be sure with a surface ECG whether the short PR interval is due to pre-excitation via an atrio-His pathway that bypasses slow conduction in the AV node or whether it is simply due to a rapidly conducting AV node. Associated arrhythmias (atrial, AV nodal and anomalous pathway dependent re-entry) are frequent in Lown–Ganong–Levine syndrome. Sudden death is very uncommon.

Mahaim-type pre-excitation

Mahaim-type pre-excitation usually presents with a normal PR interval, an LBBB-like QRS morphology and often an rS pattern in lead III [22]. A marked delta wave is usually not present. It is due to an accessory AV node connected directly to the right ventricle or is the result of an anomalous pathway linking the normal AV node to the right ventricle.

Electrocardiographic pattern of ischaemia, injury and necrosis [26–53]

The ionic changes, pathological alterations and electrophysiological characteristics that accompany different

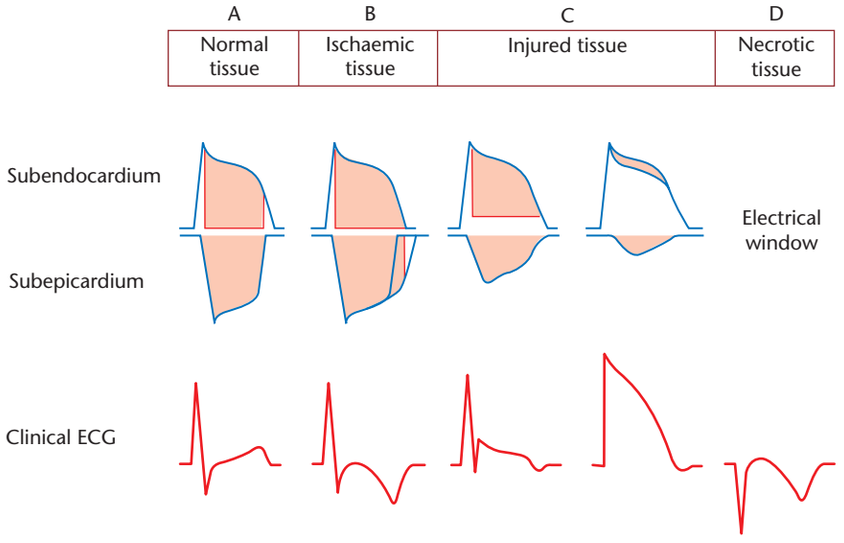

Figure 1.17 Corresponding electrical changes in subepicardial and subendocardial 'global action potentials' and the resulting ECG patterns in normal, ischaemic, injured or necrotic tissue. Correlations for normal tissue (A), subepicardial ischaemia (B), subepicardial injury (C) and necrotic tissue (D) are shown (see also Fig. 1.4).

stages of clinical ischaemia/infarction are illustrated in Fig. 1.17. The classic ECG sequence that appears in cases of complete coronary occlusion is as follows. The ECG pattern of subendocardial ischaemia (increase of T-wave amplitude) appears first. When the degree of clinical ischaemia is more important, the pattern of injury (ST-segment elevation) is present. Finally, necrosis of the myocardium is indicated by the development of a Q-wave pattern.

Electrocardiographic pattern of ischaemia

From an experimental perspective, ischaemia may be subepicardial, subendocardial or transmural. From the clinical point of view, only subendocardial and transmural ischaemia exist and the latter presents the morphology of 'subepicardial' ischaemia owing to the proximity of the subepicardium to the exploring electrode.

Experimentally and clinically, the ECG pattern of ischaemia (changes in the T wave) may be recorded from an area of the left ventricular subendocardium or subepicardium in which ischaemia induces a delay in repolarization. If the ischaemia is subendocardial, a more positive than normal T wave is recorded; in the case of subepicardial ischaemia (in clinical practice transmural), flattened or negative T waves are observed.

ALTERATIONS OF THE T WAVE DUE TO ISCHAEMIC HEART DISEASE

The negative T wave of subepicardial ischaemia (clinically transmural) is symmetric, usually with an isoelectric ST segment. It is a common finding, especially in the long term after a Q-wave myocardial infarction (Figs 1.17D and 1.18D). It may also be a manifestation of acute coronary syndrome (ACS).

The electrocardiographic pattern of ischaemia is observed in different leads according to the affected zone. In the case of inferolateral wall involvement, T-wave changes are observed in II, III, aVF (inferior leads) and/or V6, I, aVL (lateral leads). In V1–V2 (inferobasal segment),

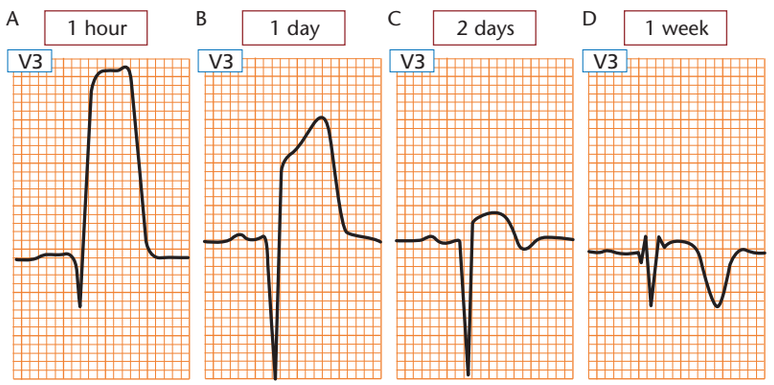

Figure 1.18 Evolutionary pattern of an extensive anterior wall myocardial infarction: (A) 1 h after the onset of pain; (B) 1 day later; (C) 2 days later; (D) 1 week later.

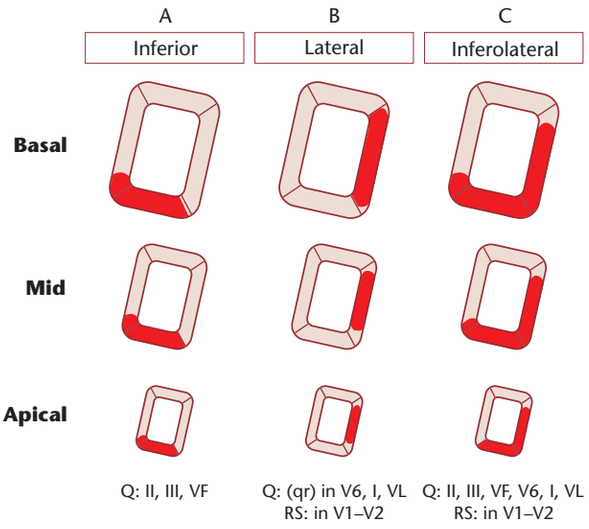

Figure 1.19 Anatomical–ECG correlations in myocardial infarction affecting (A) inferior wall, (B) lateral wall and (C) the entire inferolateral zone.

the T wave is positive instead of negative due to a mirror image (in subepicardial inferobasal injury ST depression instead of elevation, and in the case of necrosis a tall R wave instead of a Q wave) (Fig. 1.19). In anteroseptal involvement, T-wave changes are found from V1–V2 to V4–V5. If recorded in right precordial leads, it may correspond to a proximal occlusion of the left anterior descending (LAD) artery.

In contrast, an increase in T-wave amplitude, a common feature of subendocardial ischaemia, is recognized less frequently and the difficulty of diagnosis is increased because of its transient nature. It is observed in the initial phase of an attack of Prinzmetal angina (Fig. 1.20A) and occasionally in the hyperacute phase of ACS (Fig. 1.20B). Sometimes, it is not easy to be sure when a positive T wave may be considered abnormal. Therefore, sequential changes should be evaluated.

Table 1.4 Causes of a more-positive-than-normal T wave (other than ischaemic heart disease)

Normal variants: vagotonia, athletes, elderly
Alcoholism
Moderate left ventricular hypertrophy in heart diseases with diastolic overload
Stroke
Hyperkalaemia
Advanced AV block (tall and peaked T wave in the narrow QRS complex escape rhythm)

ALTERATIONS OF THE T WAVE IN VARIOUS CONDITIONS OTHER THAN ISCHAEMIC HEART DISEASE

The most frequent causes, apart from ischaemic heart disease, of a negative, flattened or more-positive-than-normal T wave are summarized in Tables 1.4 and 1.5. Examples of some of these T-wave abnormalities not due to ischaemic heart disease are shown in Fig. 1.21. Pericarditis is a very important differential diagnosis of the pattern of subepicardial ischaemia. The ECG in pericarditis shows a pattern of extensive subepicardial ischaemia with less frequent mirror images in the frontal plane, and with less negative T waves.

Electrocardiographic pattern of injury [26–36]

Experimentally and clinically, the ECG pattern of injury (changes in the ST segment) is recorded in the area of myocardial subendocardium or subepicardium where

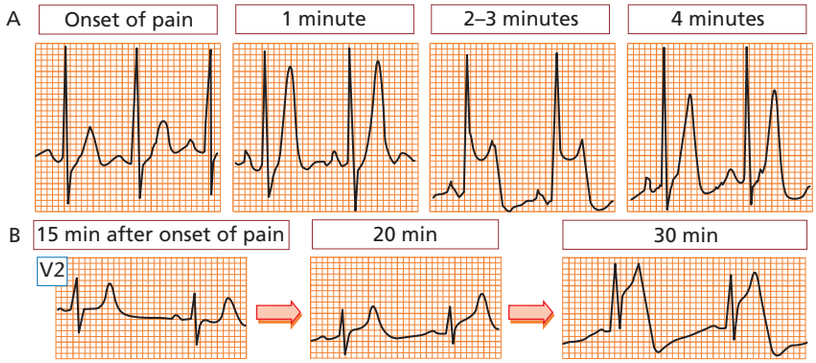

Figure 1.20 (A) Patient with Prinzmetal angina crisis: sequence of Holter ECGs recorded during a 4-min crisis. Note how the T wave becomes peaked (subendocardial ischaemia), with a subepicardial injury morphology appearing later; at the end of the crisis, a subendocardial ischaemia morphology reappears before the basal ECG returns. (B) A 45-year-old patient presenting with acute chest pain with a tall peaked T wave in right precordial leads following a normal ST segment as the only suggestive sign of acute coronary syndrome. A few minutes later, ST-segment elevation appears, followed by an increase in R wave and decrease in S wave.

Table 1.5 Causes of negative or flattened T waves (other than ischaemic heart disease)

Normal variants: children, black race, hyperventilation, females
Pericarditis
Cor pulmonale and pulmonary embolism
Myocarditis and cardiomyopathies
Alcoholism
Stroke
Myxoedema
Athletes
Medication: amiodarone, thioridazine
Hypokalaemia
Post-tachycardia
Left ventricular hypertrophy
Left bundle branch block
Post-intermittent depolarization abnormalities ('electrical memory')
Left bundle branch block
Pacemakers
Wolff–Parkinson–White syndrome

diastolic depolarization occurs as a consequence of a significant decrease in blood supply.

In the leads facing the injured zone, ST depression is recorded if the current of injury is dominant in the subendocardium (ECG pattern of subendocardial injury), while ST elevation is observed if the current of injury is subepicardial (clinically transmural) (ECG pattern of subepicardial injury). Mirror image patterns also exist, for example if subepicardial injury occurs in the posterior part of the lateral wall of the left ventricle, ST-segment elevation will be observed in the leads on the back while ST depression will be seen in V1–V2 as a mirror image. Also, the mirror images, or reciprocal changes, are very useful for locating the culprit artery and the site of the occlusion (Fig. 1.22).

The different morphologies of subepicardial injury in the evolution of acute Q-wave anterior myocardial infarction are shown in Fig. 1.18 and the various subendocardial injury ECG patterns observed in the course of an acute non-Q-wave myocardial infarction are shown in Fig. 1.23.

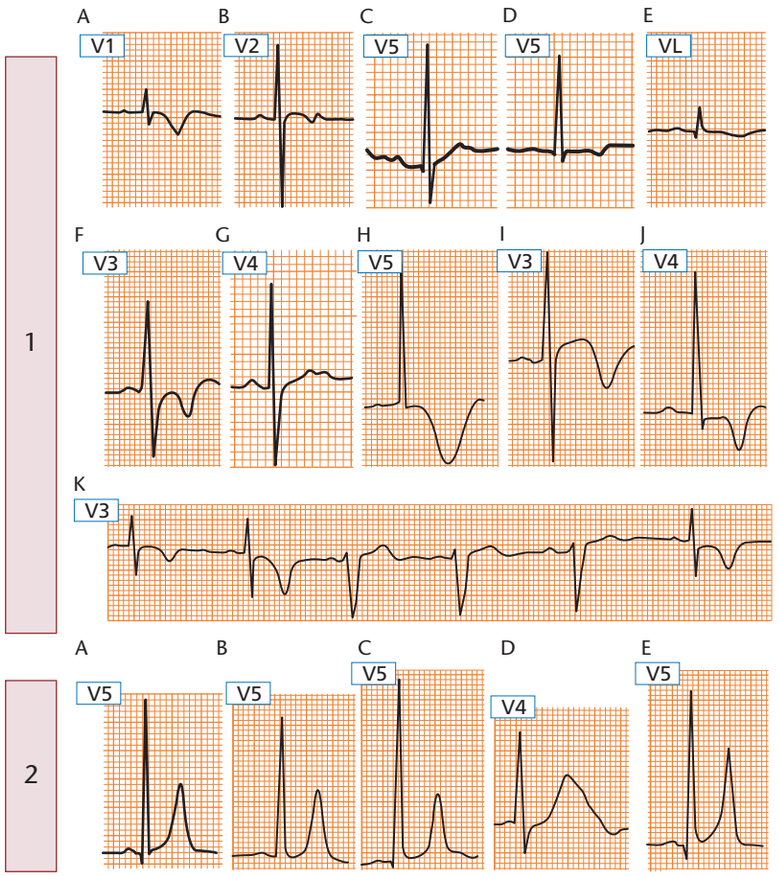

Figure 1.21 T-wave morphologies in conditions other than coronary artery disease. (1) Some morphologies of flattened or negative T waves: (A, B) V1 and V2 of a healthy 1-year-old girl; (C, D) alcoholic cardiomyopathy; (E) myxoedema; (F) negative T wave after paroxysmal tachycardia in a patient with initial phase of cardiomyopathy; (G) bimodal T wave with long QT frequently seen after long-term amiodarone administration; (H) negative T wave with very wide base, sometimes observed in stroke; (I) negative T wave preceded by ST elevation in an apparently healthy tennis player; (J) very negative T wave in a case of apical cardiomyopathy; (K) negative T wave in a case of intermittent left bundle branch block in a patient with no apparent heart disease. (2) Tall peaked T wave in (A) variant of normal (vagotonia with early repolarization), (B) alcoholism, (C) left ventricular enlargement, (D) stroke and (E) hyperkalaemia.

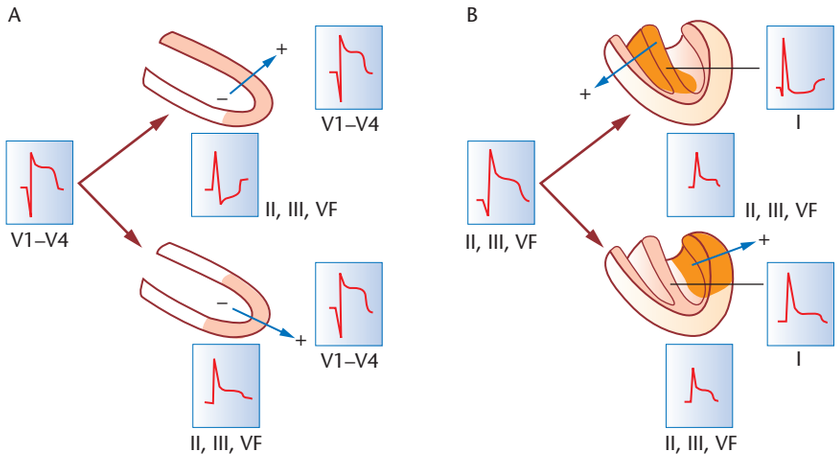

Figure 1.22 (A) ST elevation in precordial leads: as a consequence of occlusion of the left anterior descending artery (LAD), the ST changes in reciprocal leads (II, III, VF) allow identification of the site of occlusion, i.e. proximal LAD (above) shows ST depression or distal LAD (below) shows ST elevation. (B) ST elevation in inferior leads (II, III, aVF): the ST changes in other leads, in this case lead I, provide information on whether the inferior infarction is likely to be due to occlusion of the right coronary artery (above) (ST depression) or left circumflex artery (below) (ST elevation).

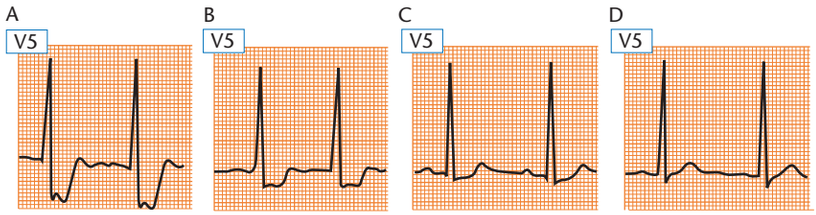

Figure 1.23 A 65-year-old patient with non-Q wave infarction. Note the evolutionary morphologies (A–D) during the first week until normalization of the ST segment.

ECG PATTERNS FOR CLASSIFICATION, OCCLUDED ARTERY IDENTIFICATION AND RISK STRATIFICATION OF ACUTE CORONARY SYNDROMES (ACS)

ACS may be classified into two types according to ECG expression: with or without ST-segment elevation. This classification has clear clinical significance as the former is treated with fibrinolysis and the latter is not. Figure 1.24 shows the different ECG presentations in ACS and their evolution.

ACS WITH ST ELEVATION [26–33]

New occurrence of ST elevation ≥ 2 mm in leads V1–V3 and ≥ 1 mm in other leads is considered abnormal and evidence of acute coronary ischaemia in the clinical setting of ACS. Sometimes minor ST elevation may be seen as a normal variant in V1–V2. Because of modern treatment, some acute coronary syndromes with ST elevation do not lead to Q-wave myocardial infarction and may not provoke a rise in enzymes. Nevertheless, the majority will develop a myocardial infarction, usually of Q-wave type (Fig. 1.24).

LAD artery occlusion leads to ST-segment elevation predominantly in precordial leads, while right coronary artery (RCA) or left circumflex (LCX) artery occlusion gives rise to ST-segment elevation in the inferior leads (Fig. 1.22). The extent of myocardium at risk can be estimated based on the number of leads with ST changes ('ups and downs') [26]. This approach has some limitations, especially related to the pseudo-normalization of ST changes in the right precordial leads that often occurs when the RCA occludes prior to the origin of the right ventricular artery.

Proximal LAD occlusion (before the first diagonal and septal arteries) as well as RCA occlusion proximal to the right ventricular artery have a poor prognosis. It is therefore useful to predict the site of occlusion in the early phase of ACS to enable decisions regarding the need for urgent reperfusion strategies. Careful analysis of ST changes in the 12-lead ECG recorded at admission may predict the culprit artery and the location of the occlusion. ST elevation is found in leads that face the head of an injury vector, while in the opposite leads ST depression can be recorded as a mirror image. Algorithms for the prediction of the sites of arterial occlusion are shown in Figs 1.25 and 1.26.

The right ventricular involvement that usually accompanies proximal RCA occlusion may be shown by ST changes in the right precordial leads (V3R, V4R) [27] (Fig. 1.26). ST-segment changes in these leads, though specific, disappear early during the evolution of myocardial infarction. Furthermore, these leads are often not recorded in emergency rooms. Thus, the real value of these changes is limited and in order to identify the culprit artery (RCA or LCX) in the case of an acute inferior myocardial infarction, we use the algorithm shown in Fig. 1.26 [31].

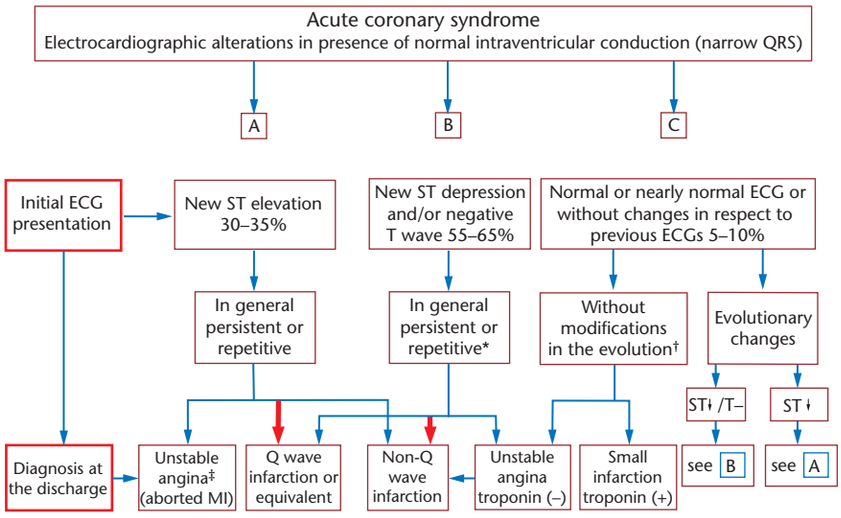

Figure 1.24 ECG alterations observed in patients with acute coronary syndrome (ACS) presenting with narrow QRS complex. Note the initial ECG presentations: (A) new ST elevation; (B) new ST depression/negative T wave; (C) normal or nearly normal ECG T wave or without changes in respect to previous ECGs. The approximate incidence of each presentation and the likely final discharge diagnosis based on both clinical and ECG settings are indicated. *In ACS with ECG pattern of ST depression or negative T waves, troponin levels allow differentiation between unstable angina (troponin negative) and non-Q-wave infarction (troponin positive). Usually, cases with short-duration ECG changes, particularly with negative T waves, present with negative troponin levels and correspond to unstable angina. †According to ESC/ACC guidelines in patients presenting with chest pain or its equivalent suggestive of ACS with accompanying normal ECG, troponin level is a key factor in differentiating between small myocardial infarction (MI) and unstable angina. ‡Sometimes, thanks to quick treatment, patients present with normal troponin levels despite important ST elevation in the initial ECG (aborted MI).

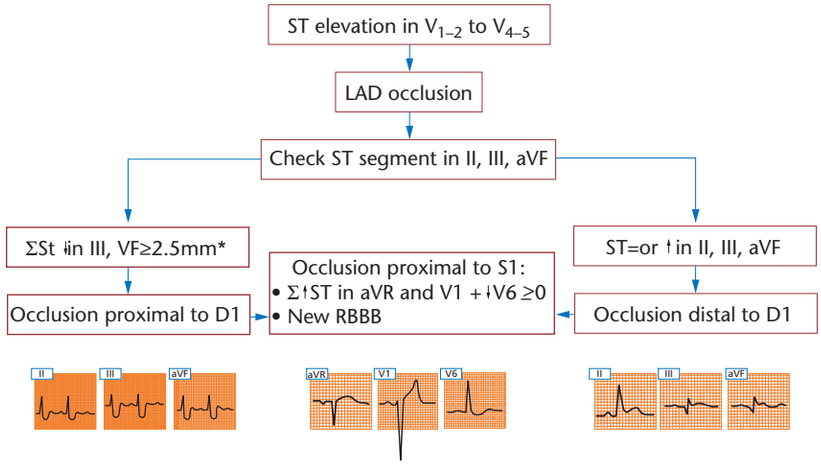

Figure 1.25 Algorithm for locating occlusion of left anterior descending artery (LAD) in evolving myocardial infarction with ST elevation (STEMI) in precordial leads, with ECG examples of the different situations. *Cases with ST depression < 2.5 mm are the most difficult to classify.

Furthermore, the criterion of isoelectric or elevated ST in V1 has the highest accuracy in predicting proximal RCA occlusion [32]. In these cases the ST elevation in V1 may also occur in V2 or V4 but with a V1/V3–4 ratio over 1. This differentiates these cases from cases of antero-inferior infarction [33], in which there is also ST elevation in inferior and precordial leads but the ST elevation V1/V3–4 ratio is less than 1.

ACS WITHOUT ST ELEVATION

ACS with ST depression in eight or more leads has a worse prognosis as it frequently corresponds to a left main artery subocclusion or its equivalent (three-vessel disease). Generally, in these cases ST elevation in aVR can be observed as a mirror image [34] (Fig. 1.27). If, in cases of ACS without ST elevation, ST depression in V4–V5 is followed by a final positive T wave, the prognosis is better

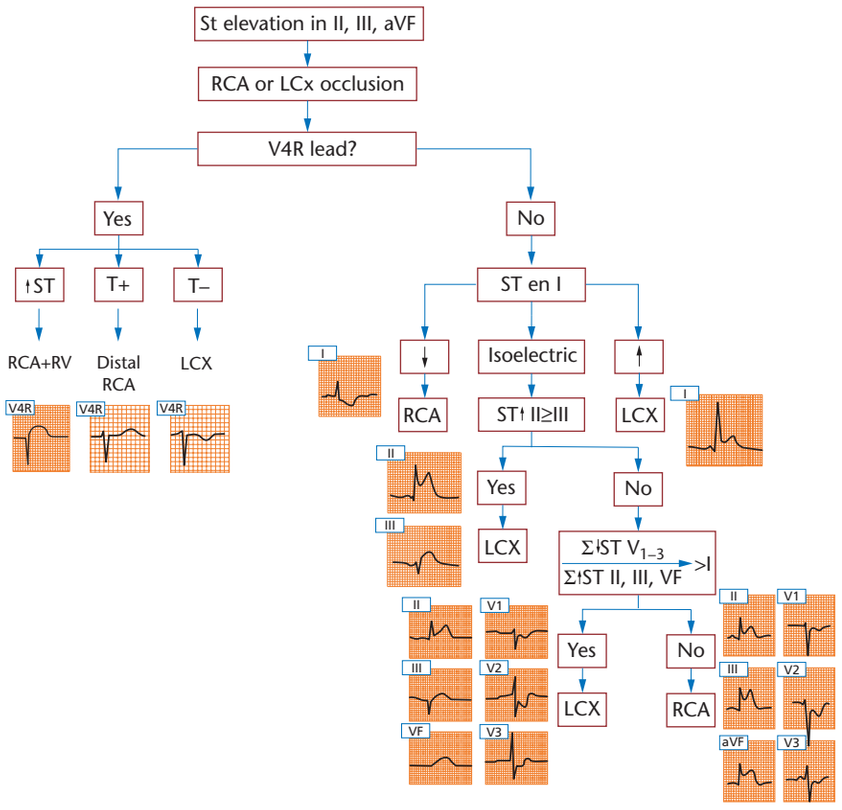

Figure 1.26 Algorithm for locating occlusion of right coronary artery (RCA) or left circumflex artery (LCx) in evolving myocardial infarction with ST elevation (STEMI) in inferior leads, with ECG examples of different situations.

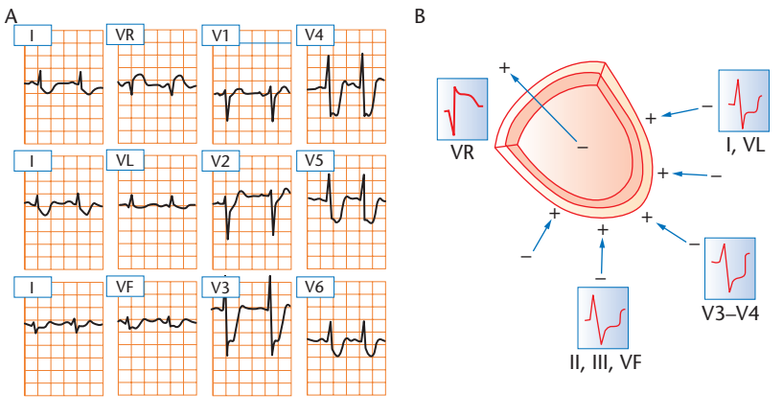

Figure 1.27 (A) ST-segment depression in more than eight leads and ST-segment elevation in VR in a case of non-STEMI due to involvement of the left main coronary artery. Note that the maximum depression occurs in V3–V4 and ST-segment elevation occurs in aVR as a mirror image. (B) Schematic representation that explains how ST-segment depression is seen in all leads, except for aVR and V1, in a case of non-Q-wave infarction secondary to the involvement of the left main coronary artery. The vector of circumferential subendocardial injury is directed from the subepicardium to the subendocardium and is seen as a negative vector in all leads except VR.

and single-vessel (often the proximal LAD) disease may be present [35]. The presence of deep negative T waves from V1 to V4–V5 suggests subocclusion of the proximal LAD. On the other hand, in the group of ACS with ST depression and/or negative T waves, the presence in leads with dominant R waves of mild ST depression usually signifies a worse prognosis than negative T waves.

ST-SEGMENT ALTERATIONS REMOTE FROM THE ACUTE PHASE OF ISCHAEMIC HEART DISEASE

ST-segment elevation is usually found in association with coronary spasm (Prinzmetal angina) often preceded by peaked and tall T waves [36] (see Fig. 1.20A). Occasionally, upward convex ST elevation may persist after the acute phase of a myocardial infarction. It has been

Table 1.6 Most frequent causes of ST-segment elevation (other than ischaemic heart disease)

Normal variants: chest abnormalities, early repolarization, vagal overdrive. In vagal overdrive, ST-segment elevation is mild and generally accompanies the early repolarization image. T wave is tall and asymmetric
Athletes: sometimes an ST-segment elevation exists that may even mimic an acute coronary syndrome with or without negative T waves, at times prominent. No coronary involvement has been found, although this abnormality has been observed in sportsmen who die suddenly; thus its presence implies the need to exclude hypertrophic cardiomyopathy
Acute pericarditis in its early stage and myopericarditis
Pulmonary embolism
Hyperkalaemia: the presence of a tall peaked T wave is more evident than the accompanying ST-segment elevation, but sometimes it may be evident
Hypothermia
Brugada's syndrome
Arrhythmogenic right ventricular cardiomyopathy
Dissecting aortic aneurysm
Left pneumothorax
Toxicity secondary to cocaine abuse, etc.

classically considered to be related to left ventricular aneurysm. The specificity of this sign is high but its sensitivity is low. On the other hand, slight persistent ST-segment depression is frequently observed in coronary disease due to persistence of ischaemia. An exercise test may increase this pattern.

ST-segment alterations in conditions other than ischaemic heart disease

Different causes of ST-segment elevation, aside from ischaemic heart disease, are shown in Table 1.6. Representative examples are illustrated in Fig. 1.28. The most frequent causes of ST-segment depression in situations other than ischaemic heart disease are shown in Table 1.7.

Electrocardiographic pattern of necrosis [37–53]

Classically, the electrocardiographic pattern of established necrosis is associated with a pathological Q wave, generally accompanied by a negative T wave (necrosis Q wave) [1] (Table 1.8). The specificity of this criterion is high but its sensitivity is low (around 60%) and is even lower with current treatment regimens and the new definition of myocardial infarction (ESC/ACC consensus) [37,38].

Table 1.7 Most frequent causes of ST-segment depression (other than ischaemic heart disease)

Normal variants: sympathetic overdrive, neurocirculatory asthenia, hyperventilation
Medications: diuretics, digitalis
Hypokalaemia
Mitral valve prolapse
Post-tachycardia
Secondary: bundle branch block, ventricular hypertrophy

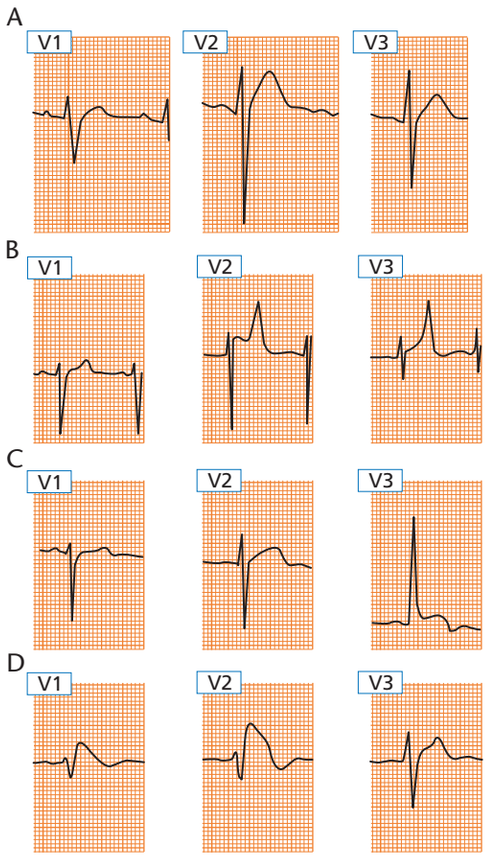

Figure 1.28 The most frequent causes of ST elevation other than ischaemic heart disease: (A) pericarditis; (B) hyperkalaemia; (C) in athletes; (D) Brugada pattern.

Figure 1.18 shows the ECG morphology seen with transmural involvement after total occlusion of a coronary artery. After an initial stage of ST-segment elevation, a Q wave with a negative T wave appears. It was thought that cases of non-Q-wave infarction had a predominantly subendocardial location (electrically 'mute'). Thus, it was considered that Q-wave infarction signified transmural involvement, while non-Q-wave infarction implied subendocardial compromise.

It is now well known that, from a clinical point of view, isolated subendocardial infarctions do not exist [39]. Nevertheless, there are infarctions that compromise a great portion of the wall, but with subendocardial predominance, which may or may not develop a Q wave. Furthermore, there are completely transmural infarctions (such as infarctions of basal parts of the cardiac

Table 1.8 Characteristics of the pathological Q wave, named 'necrosis Q wave' when secondary to myocardial infarction

Characteristics of pathological Q wave

Duration: ≥ 30 ms in I, II, III, aVL and aVF, and in V3–V6. The presence of a Q wave is normal in aVR. In V1–V2, all Q waves are pathological. Usually also in V3, except in cases of extreme laevo-rotation (qRs in V3)

Depth: above the limit considered normal for each lead, i.e. generally 25% of the R wave (frequent exceptions, especially in aVL, III and aVF)

Present even a small Q wave in leads where it does not normally occur (e.g. qrS in V1–V2)

Q wave with decreasing voltage from V3–V4 to V5–V6, especially if accompanied by a decrease of voltage in R wave compared with previous ECG

Criteria for diagnosing location of myocardial infarction

Anteroseptal zone

Q wave, regardless of duration and depth, in V1–V3

Presence of Q wave > 30 ms in duration and over 1 mm in depth in leads I, aVL, V4–V6

Inferolateral zone

Presence of Q wave in II and aVF; lead III is not used due to false-positive cases

Q wave may appear in lateral leads (V6 or V6 and/or I and aVL)

ECG may present equivalent of Q wave (increase in R wave in V1–V2) or be practically normal in cases of involvement of posterior part of lateral wall

walls, especially the posterior part of the lateral wall) that may not develop a Q wave. This assumption has been recently confirmed by magnetic resonance imaging (MRI) [40]. Consequently, the distinction between transmural (Q-wave infarction) and subendocardial (non-Q-wave infarction) can no longer be supported.

Q-WAVE INFARCTION

Genesis of Q Wave The appearance of the Q wave of necrosis may be explained by the electrical window theory of Wilson (Fig. 1.29). The vector of necrosis is equal in magnitude but opposite in direction to the normal vector that would be generated in the same zone without necrosis. The onset of ventricular depolarization changes when the necrotic area corresponds to a zone that is depolarized within the first 40 ms of ventricular activation, which applies to the majority of the left ventricle except the posterobasal parts.

Location of infarction In everyday practice the nomenclature of the affected myocardial infarction zone is still determined by the presence of Q waves in different leads as proposed more than 50 years ago by Myers *et al*. [41]

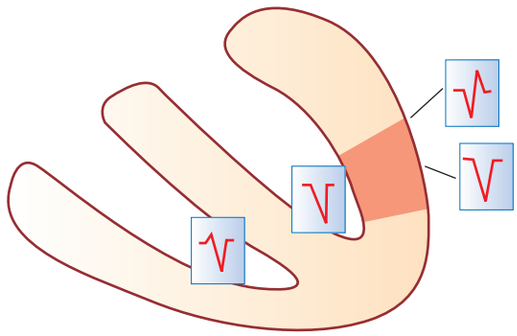

Figure 1.29 According to Wilson the necrotic zone is an electrical window that allows the intraventricular normal QS morphology to be recorded from the opposing necrotic wall of the left ventricle. The lead facing the necrotic myocardium 'looks' into the cavity of the left ventricle.

based on their classical pathological study. According to this classification, the presence of Q waves in V1–V2 represents septal infarction, in V3–V4 anterior infarction, in V1–V4 anteroseptal infarction, in V5–V6 low lateral infarction, in V3–V6 anterolateral infarction, in V1–V6 anteroseptolateral infarction, and in I and aVL high lateral infarction.

However, this classification has some limitations. Correlation with coronary angiography and imaging techniques including MRI [42–46] has revealed the following.

1. The presence of a Q wave in V1–V2 does not imply involvement of the entire septal wall; as a matter of fact the initial vector of ventricular depolarization originates in the mid-low part of the anterior septum. Therefore, the upper part of the septum need not be involved for the appearance of a Q wave in V1–V2.
2. Correlation with cardiovascular magnetic resonance (CE-CMR) [45,46] has demonstrated that: (a) the posterior wall often does not exist, therefore the basal part of the inferior wall should be called the inferobasal segment (segment 4); (b) the necrosis vector (NV) of the inferobasal segment faces V3–V4 and not V2–V1, therefore the RS morphology does not originate in V1; in those cases where the inferobasal segment does not bench upwards (the entire inferior wall is flat), the NV is directed only upwards and contributes to the Q wave in II, III and VF; (c) in cases of isolated lateral infarction, the NV may face V1, explaining the RS morphology seen in this lead.
3. In rare cases, if the LAD is very long, the occlusion of this artery proximal to S1 and D1 may not cause Q waves in I and aVL because the vector of necrosis of the lateral wall may be masked by the vector of necrosis of the inferior wall.
4. Because of new treatments for revascularization given

Type of MI		Infarction area (CMR)	ECG pattern	Name given to MI	Most probable place of occlusion
ANTEROSEPTAL ZONE	A1 n=7	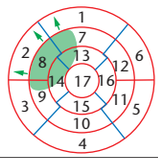	Q in V1–2 SE: 86% ES: 98%	Septal	
	A2 n=7	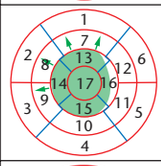	Q in V1–2 to V4–V6 SE: 86% ES: 98%	Apical/ anteroseptal	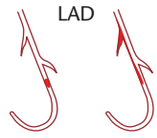
	A3 n=6	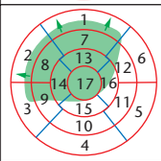	Q in V1–2 to V4–V6 I and VL SE: 83% ES: 98%	Extensive anterior	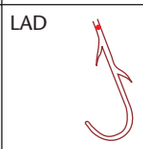
	A4 n=4	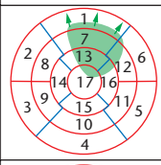	Q (qs or r) in VL (I) and sometimes V2–3 SE: 70% ES: 100%	Limited anterior	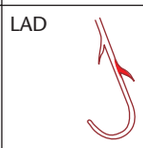
INFEROLATERAL ZONE	B1 n=6	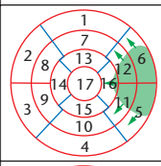	Q (qr or r) in I, VL, V5–6 and/or RS in V1 SE: 50% ES: 98%	Lateral	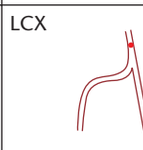
	B2 n=8	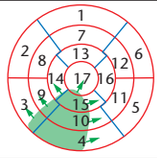	Q in II, III, VF SE: 87.5% ES: 98%	Inferior	
	B3 n=10	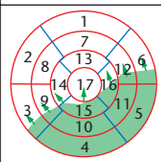	Q in II, III, VF (B2) + Q in I, VL, V5, 6 and / or RS in V1 (B1) SE: 70% ES: 100%	Inferolateral	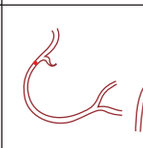

Figure 1.30 Relationship between infarcted area, ECG pattern, name given to infarction and the most probable culprit artery and place of occlusion. LAD, left anterior descending artery; RCA, right coronary artery; LCX, left circumflex artery.

in the acute phase, the necrotic zone is often very limited compared with the zone at risk in the acute phase.

5 The location of precordial, especially mid-precordial (V3–V5), leads may change from one day to another and therefore it is difficult to make a diagnosis based on the presence or absence of Q waves in these leads.

As a result of these limitations, a study on correlations between ECG patterns and different myocardial areas of necrosis detected by CMR has been undertaken in the chronic phase of myocardial infarction [45,46]. The left ventricle was divided into two zones, anteroseptal and inferolateral. Figure 1.30 shows seven ECG patterns that accurately correlate with seven areas of necrosis detected on CMR (four anteroseptal and three inferolateral) (see also Figs 1.31 and 1.32). Nevertheless, some areas, especially at the base, frequently present with normal ECGs in the chronic phase [46].

Quantification A quantitative QRS score has been developed by Selvester *et al.* [47] to estimate the extent of myocardial necrosis especially in the case of anterior myocardial infarction. Recently, the same group demonstrated that MRI may improve its accuracy [48]. The most significant error was the misinterpretation of Q waves in V1–V2 as indicating basal septal and anterior wall

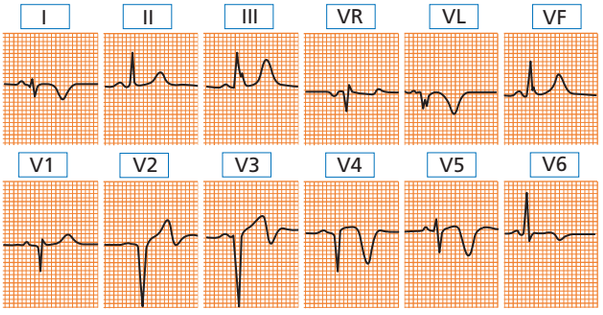

Figure 1.31 ECG of extensive anterior myocardial infarction (A3 type in Fig. 1.30).

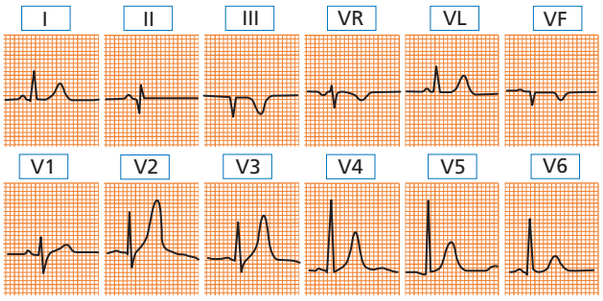

Figure 1.32 ECG of inferolateral myocardial infarction (B3 type in Fig. 1.30).

involvement. As already stated this is incorrect because the first vector (r wave in V1–V2) is generated in the mid-low anterior part of the septum. Also recently, it has been found that pre-discharge scoring in patients with anterior Q waves did not correlate with the amount of myocardial damage as estimated by radionuclide techniques in patients treated with and without thrombolytics [49]. Furthermore, spontaneous changes in the QRS score from discharge to 6 months seem to be of limited value in identifying patients with late improvement of perfusion or left ventricular function.

Differential diagnosis of pathological Q wave

Although the specificity of a pathological Q wave for diagnosing myocardial infarction is high, similar Q waves can be seen in other conditions. The diagnosis of myocardial infarction is based not only on electrocardiographic alterations but also on the clinical evaluation and enzyme changes. The pattern of ischaemia or injury accompanying a pathological Q wave is supportive of the Q wave being secondary to ischaemic heart disease. The main causes of pathological Q waves other than myocardial necrosis are listed in Table 1.9. On the other hand, in 5–25% of Q-wave infarctions (with the highest incidence in inferior wall infarction) the Q wave disappears with time, which explains the relatively poor sensitivity of the Q wave for detecting old myocardial infarction.

Table 1.9 Pathological Q wave not secondary to myocardial infarctioon

During the evolution of an acute disease involving the heart
Acute coronary syndrome with an aborted infarction
Coronary spasm (Prinzmetal angina type)
Acute myocarditis
Presence of transient apical dyskinesia that also shows ST-segment elevation and a transient pathological q wave (Tako-tsubo syndrome) [53]
Pulmonary embolism
Miscellaneous: toxic agents, etc.
Chronic pattern
Recording artefacts
Normal variants: aVL in the vertical heart and III in the dextrorotated and horizontal heart
QS in V1 (hardly ever in V2) in septal fibrosis, emphysema, the elderly, chest abnormalities, etc.
Some types of right ventricular hypertrophy (chronic cor pulmonale) or left ventricular hypertrophy (QS in V1–V2, or slow increase in R wave in precordial leads, or abnormal q wave in hypertrophic cardiomyopathy)
Left bundle branch conduction abnormalities
Infiltrative processes (e.g. amyloidosis, sarcoidosis, tumours, chronic myocarditis, dilated cardiomyopathy)
Wolff–Parkinson–White syndrome
Dextrocardia
Phaeochromocytoma

Diagnosis of necrosis in the presence of ventricular blocks, pre-excitation or ventricular pacemaker

Complete RBBB Since cardiac activation begins normally in RBBB, the presence of a myocardial infarction causes an alteration in the first part of the QRS complex that can generate a Q wave, just as with normal ventricular conduction. Furthermore, in the acute phase the ST–T changes can be seen exactly as with normal activation. Patients with ACS with ST elevation that during its course develops new-onset complete RBBB usually have the LAD occluded before the first septal and first diagonal arteries (Fig. 1.25). This is explained by the fact that the right bundle branch receives its blood supply from the first septal artery.

Complete LBBB In the acute phase, the diagnosis of myocardial infarction in the presence of complete LBBB may be suggested by ST-segment changes [50]. In the chronic phase, detection of underlying myocardial infarction is difficult. Ventricular depolarization starts close to the base of the anterior papillary muscle of the right ventricle. This causes a depolarization vector that is directed forward, downwards and to the left. Trans-septal depolarization of the left ventricle initiates subsequent

vectors. As a result, even if important zones of the left ventricle are necrotic, the overall direction of the initial depolarization vector does not change and it continues to point from right to left, preventing the inscription of a Q wave. Nevertheless, small 'q' waves or tall R waves may occasionally be observed [6]. The correlation of clinical and ECG changes with enzyme changes and radionuclide studies have confirmed that the presence of Q waves in I, aVL, V5 and V6 and R waves in leads V1–V2 are the most specific criteria for diagnosing myocardial infarction in the presence of LBBB in the chronic phase [51].

Diagnosis of Q-wave myocardial infarction in the presence of a hemiblock In general, necrosis associated with LAH may be diagnosed without difficulty. In the case of an ECG with left-axis deviation of the QRS and Q waves in II, III and aVF, the presence of QS without a terminal 'r' wave confirms the association with LAH. In some cases, mainly in small inferior myocardial infarctions, LAH may mask myocardial necrosis. The initial vector is directed more downwards than normal as a result of LAH and masks any necrosis vector due to a small inferior myocardial infarction.

LPH may mask or decrease an inferior necrosis pattern by converting a QS or Qr morphology in II, III and aVF into QR or qR pattern. It may also cause a small positive wave in I and aVL in the case of a lateral myocardial infarction because the initial vector in LPH may be directed more upwards than usual as a result of LPH and mask the necrosis vector of a small lateral infarction.

Pre-excitation and pacemakers It is difficult to diagnose myocardial infarction in the presence of pre-excitation. Sometimes it may be suggested by changes of repolarization especially in the acute phase of ACS. Also, in patients with pacemakers the changes in repolarization, especially ST elevation, may suggest ACS [52]. In the chronic phase of myocardial infarction the presence of a spike qR pattern, especially in V5–V6, is a highly specific but poorly sensitive sign of necrosis.

Value of the ECG in special conditions [1,4,14]

The most characteristic ECG patterns in different clinical conditions, such as electrolyte imbalance, hypothermia and in athletes, are shown in Fig. 1.33.

ECG patterns associated with sudden cardiac death

Figure 1.34 shows the most characteristic ECG patterns in genetically induced conditions that may trigger sudden death, such as long QT syndrome, Brugada's syndrome and arrhythmogenic right ventricular dysplasia. Hypertrophic cardiomyopathy is often associated with an ECG showing left ventricular hypertrophy without clear differentiation from other causes of left ventricular hypertrophy. However, a typical ECG pattern is sometimes present (Fig. 1.34).

ECG of macroscopic electrical alternans [1]

Alternans of ECG morphologies is diagnosed when there are repetitive changes in the morphology of alternate QRS complexes, ST segments or rarely P waves. The presence of definite QRS alternans during sinus rhythm

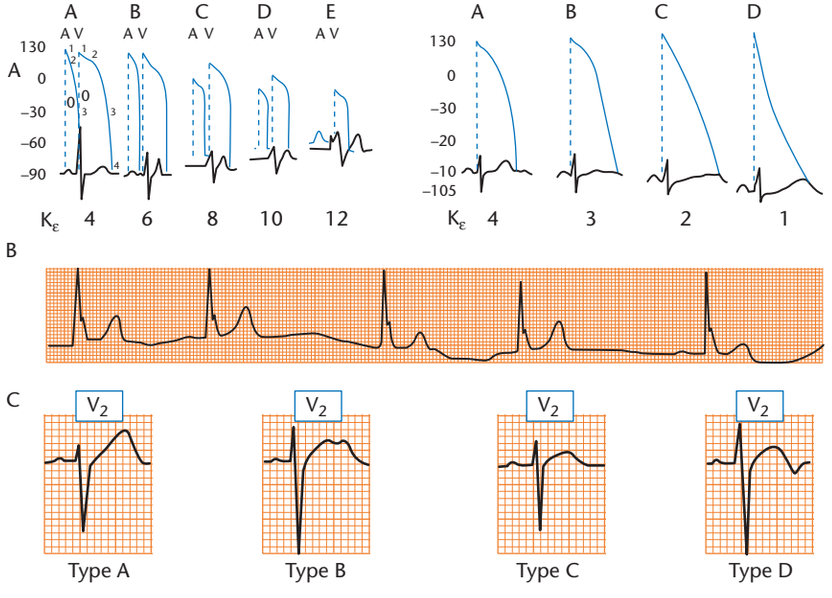

Figure 1.33 ECG patterns in (A) hyperkalaemia and hypokalaemia (see different patterns at different levels of K^+); (B) hypothermia (note the Osborne or 'J' wave at the end of the QRS and bradycardia with different repolarization abnormalities); (C) athletes without evidence of heart disease.

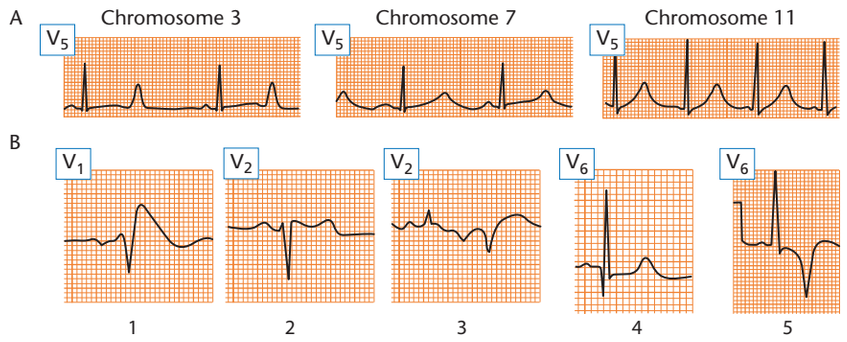

Figure 1.34 Other ECG patterns associated with sudden cardiac death. (A) Long QT syndrome related to genetic abnormalities on chromosomes 3, 7 and 11. (B1,2) The Brugada pattern: (1) typical, with coved ST elevation; (2) atypical, with wide r' and 'saddleback' ST elevation (also a possible normal variant). (B3) Arrhythmogenic right ventricular cardiomyopathy. Note the atypical complete right bundle block, negative T waves in V1–V4 and premature ventricular impulses from the right ventricle. QRS duration is much longer in V1 than in V6. (B4) Typical pattern of a pathological Q wave in a patient with hypertrophic cardiomyopathy. (B5) Typical ECG pattern from a patient with hypertrophic apical cardiomyopathy.

may occasionally be observed in mid-precordial leads, particularly in very thin subjects during respiration. True alternans of QRS complexes (change in morphology without change of width) is suggestive of a large pericardial effusion and sometimes cardiac tamponade (Fig. 1.35A). Alternans of QRS morphology may also be observed during supraventricular arrhythmias, especially in patients with WPW syndrome. True alternans of

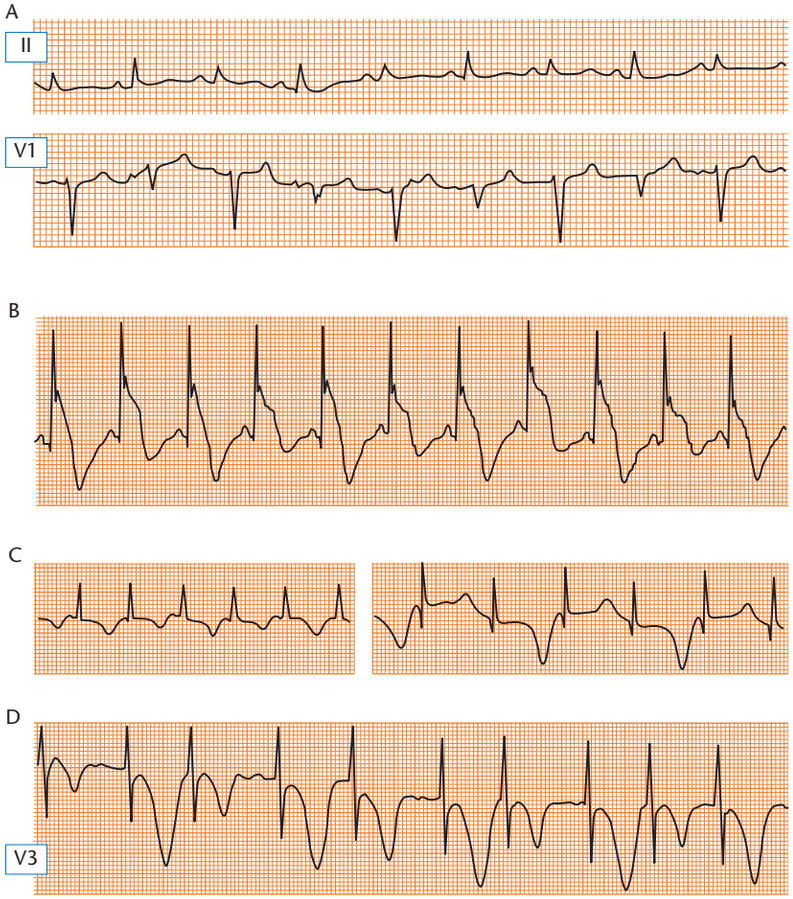

Figure 1.35 Typical examples of electrical alternans: (A) alternans of QRS in a patient with pericardial tamponade; (B) ST–QT alternans in Prinzmetal angina; (C) repolarization alternans in congenital long QT syndrome; (D) repolarization alternans in significant electrolyte imbalance.

QRS complexes can be confused with QRS changes, such as alternating bundle branch block or WPW pattern, with normal conduction. In these situations, two clearly distinct QRS–T morphologies exist with different QRS widths and sometimes with changes in the PR interval.

Alternans of the ST–T components of the ECG may be observed in the hyperacute phase of severe myocardial ischaemia (Fig. 1.35B), in congenital long QT syndrome (Fig. 1.35C) and with significant electrolyte imbalance (Fig. 1.35D). Techniques now exist to detect microvolt T-wave alternans, which are potentially important for risk stratification [54–57].

Incorrect electrode placement and cable connection

Reversal of the left arm, right arm or left leg electrode

The most common technical errors are incorrect cable connections to the peripheral electrodes. Table 1.10 presents the changes in the peripheral leads resulting from incorrect connection of the right arm, left arm and left leg electrode cables.

Most frequently, the left arm and right arm electrode cables are reversed. The mistake is easily recognizable during sinus rhythm by the presence of a negative P wave in lead I in the absence of other ECG signs of dextrocardia, such as mostly negative QRS complexes in leads V3–V6 (Fig. 1.36) [58]. The T wave may or may not be inverted depending on the underlying pathology. In the presence of atrial fibrillation, if the QRS complex in lead I is inverted compared with the QRS in lead V6, the arm electrodes have likely been reversed [59].

Reversal of the right arm and left leg electrode cables produces an ECG pattern that might resemble inferior myocardial infarction as aVF has the appearances of aVR. This technical error can also be suspected from an inverted P wave in aVF.

Reversal of the left arm and left leg electrodes is difficult to recognize, unless a previously recorded ECG is available for comparison [58–60]. In the presence of some ECG abnormalities, this technical error might be more easily suspected than in a normal ECG, e.g. during atrial flutter by the appearance of saw-tooth flutter waves in leads I, III and aVL but not lead II [58].

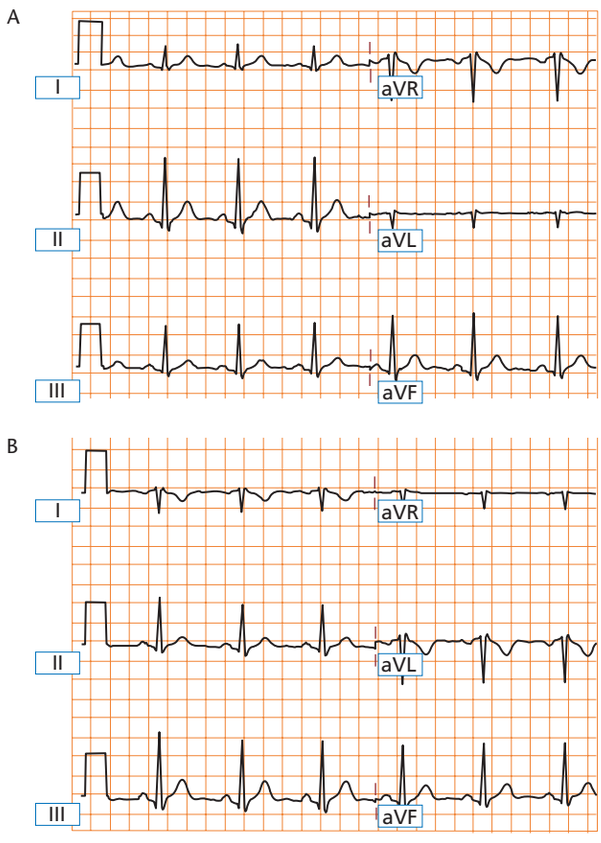

Figure 1.36 Limb leads of a 12-lead ECG recorded with correct cable connections (A) and after intentional reversal of the left arm and right arm electrode cables (B).

Table 1.10 Changes in the six peripheral leads resulting from errors in connecting the right arm, left arm and left leg cables

	Lead*					
Reversal	**'I'**	**'II'**	**'III'**	**'aVR'**	**'aVL'**	**'aVF'**
Left arm–right arm	Inverted I	III	II	aVL	aVR	Unchanged
Left arm–left leg	II	I	Inverted III	Unchanged	aVF	aVL
Right arm–left leg	Inverted III	Inverted II	Inverted I	aVF	Unchanged	aVR

*The leads as they appear in the ECG recorded with wrong connections.

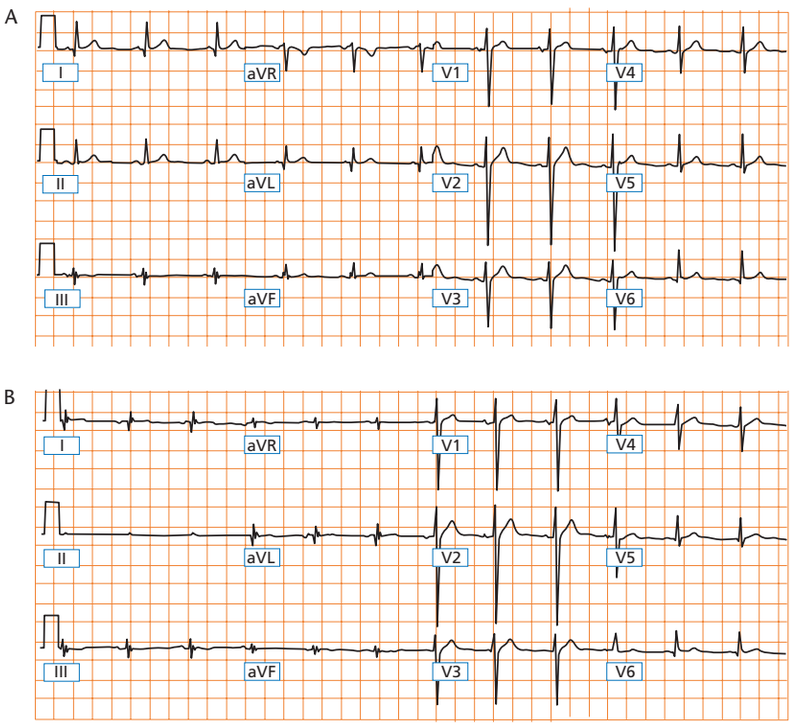

Figure 1.37 Standard 12-lead ECG recorded with correct cable connections (A) and after intentional reversal of the right arm and right leg electrode cables (B).

Incorrect connections of the right leg (ground) electrode

The ground electrode, which is placed on the right leg by convention, can be positioned anywhere on the body without affecting the ECG waveforms. However, when the ground electrode cable is interchanged with the right arm or left arm electrode cables, significant changes occur in both the morphology and amplitude of most peripheral leads [58–61]. Three possible lead reversals are of practical importance: right arm–right leg reversal (the most frequent), left arm–right leg reversal, and interchange of both leg cables with the corresponding arm cables. Reversal of the right and left leg electrodes does not change the ECG noticeably, because the potential at both legs is practically the same.

The hallmark of these misplacements is that one standard lead (I, II or III) shows almost a straight line (potential difference between both legs). When the right arm and right leg cables are reversed, this is seen in lead II (Fig. 1.37), whereas with left arm and right leg cable reversal, it is seen in lead III. Likewise, when both leg electrode cables are switched with the corresponding arm cables, lead I shows a very low potential [61]. Importantly, the central terminal is affected by these three connection errors. This may lead to visible changes in the precordial leads [58].

Errors in connection of precordial electrodes

Interchange of precordial cables is a common technical error that is usually easy to spot. It may be suspected if the transition of the P wave, QRS complex and T wave is unexplainable [58], for example lower amplitude of R wave and deeper S wave in V3 compared with V2 when V2 and V3 cables are reversed, or lack of the normal increase in amplitude of the T wave from V2 to V3 to V4, etc. [59].

Incorrect electrode placement

Incorrect (and hence most likely variable and inconsistent) placement of the precordial electrodes is a well-recognized and important source of inaccuracy [62]. It has been repeatedly shown that a change in the precordial electrode positions by as little as 2 cm can produce diagnostically important differences [63–65]. For example, Herman *et al*. [65] have demonstrated that even a 2-cm vertical displacement of the precordial electrodes produced a greater than 25% change in R-wave amplitude in half of their patients, leading to altered R-wave progression in 20% of patients and a shift in the precordial transition zone in 75%.

Precordial electrode displacement of such magnitude often occurs even when experienced clinicians or ECG

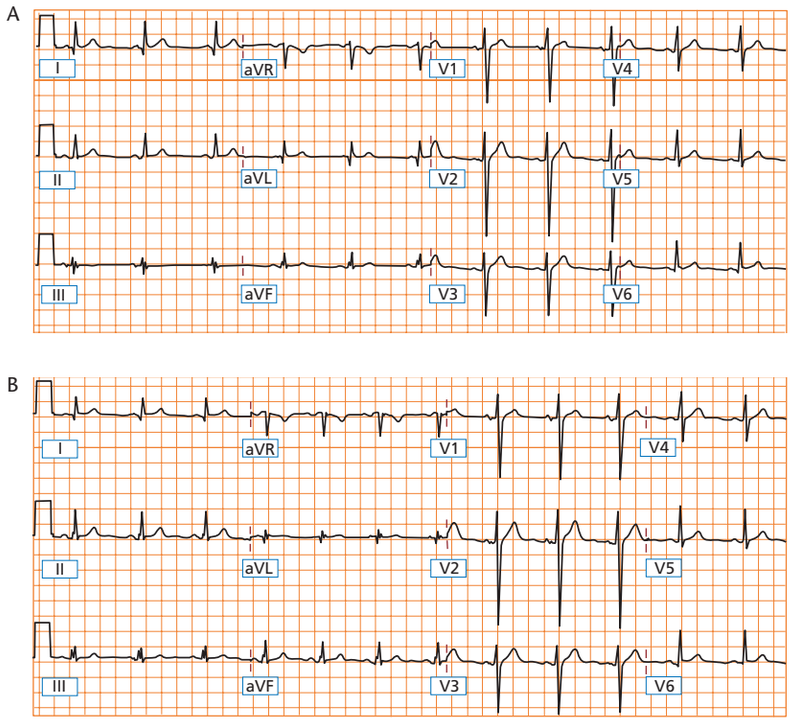

Figure 1.38 Standard 12-lead ECG recorded with the peripheral electrodes in the standard position (A) and positioned according to the Mason–Likar system (B).

technicians are recording the ECG [66,67]. Frequent mistakes include positioning V1 and V2 too high, in the third and even in the second instead of the fourth intercostal space, with resultant vertical misplacement of all precordial leads, excessively wide separation of V1 and V2, and placement of V4 and V5 too low and too lateral [66]. When V1 and V2 are placed one or more intercostal spaces higher, they tend to show an rSr′ configuration with inverted P and T waves, resembling incomplete RBBB.

There is still no universal agreement [68–70] about whether the precordial electrodes in female patients should be placed underneath or on top of the left breast. However, when the electrodes are placed over the left breast instead of beneath it, they are likely vertically displaced. In general submammary placement is recommended.

It is common practice in many centres to attach the arm electrodes above the wrists (forearms, upper arms) or above the ankles, in the belief either that it makes no difference where exactly on the limb they are placed or that it decreases the noise. However, it has been shown that there is a small potential difference between the upper arm and the wrists [59–71], and a similar potential difference is likely to exist between the ankles and the upper leg. However, these differences are hardly noticeable to the naked eye and will not affect the clinical (visual) interpretation of the ECG, hence the recommendation of the American Heart Association that 'the electrodes may be placed on any part of the arms or of the left leg as long as they are below the shoulders in the former and below the inguinal fold anteriorly and the gluteal fold posteriorly in the latter' [72].

In exercise electrocardiography and recently in 12-lead ambulatory (Holter) electrocardiography the Mason–Likar electrode system [73] is used, in which the limb leads are moved onto the torso. There are very significant differences between the conventional 12-lead ECG and one recorded using the Mason–Likar electrode system, including rightward shift of the mean QRS axis, reduction of R-wave amplitude in leads I and aVL and significant increase in R wave in leads II, III and aVF (Fig. 1.38). The precordial leads are also affected because of the altered potential of the central terminal [74].

Ventricular signal-averaged electrocardiography

Signal-averaged electrocardiography (SAECG) is the most widely used method of high-resolution electrocardiography and aims to record cardiac signals from

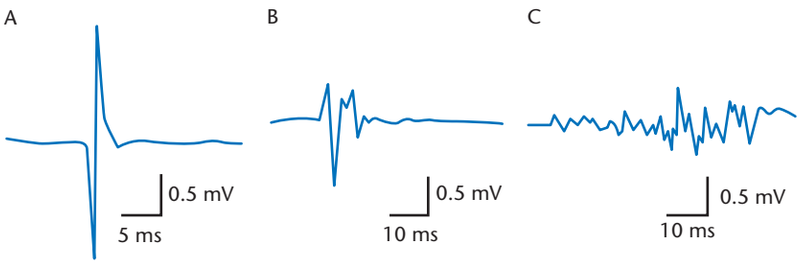

Figure 1.39 Development of low-amplitude fractionated electrograms in experimental models of myocardial infarction in canine hearts. Bipolar subepicardial electrograms are shown recorded from (A) a non-infarcted preparation, (B) 5-day-old infarction and (C) 2-month-old infarction. The low-amplitude fractionated electrograms shown in (C) reflect zones of abnormal conduction, which represent a substrate for the development of re-entrant arrhythmias. These can be recorded as late potentials on the signal-averaged ECG. Reproduced with permission from Gardner *et al*. [80].

the body surface that are not visible or apparent from the standard ECG [75]. In its most popular form, ventricular SAECG uses temporal averaging in order to improve the signal-to-noise ratio and enable the detection of low-amplitude potentials usually outlasting the QRS complex (so-called 'late potentials') [75–77]. Late potentials on SAECG reflect low-amplitude fractionated electrograms generated by surviving myocardial fibres within or surrounding regions of myocardial infarction (less frequently by other forms of ischaemic heart disease or other cardiac diseases) that are activated after a delay and thus create a substrate for re-entrant ventricular arrhythmias (Fig. 1.39) [78–80].

The SAECG is recorded using orthogonal bipolar XYZ ECG leads, which are averaged, filtered and combined into a vector magnitude called the filtered QRS complex. The most frequently used time-domain analysis (Fig. 1.39) of the filtered QRS complex includes:

1 filtered QRS duration;
2 root-mean-square voltage of the terminal 40 ms of the filtered QRS (RMS40);
3 duration that the filtered QRS complex remains < 40 μV (LAS).

The abnormal SAECG recorded with a 40-Hz high-pass filter (i.e. the presence of late potentials) is characterized by a filtered QRS complex > 114 ms, RMS40 < 20 μV and LAS > 38 ms [76,81], of which the most important is the prolonged filtered QRS duration (Figs 1.40 and 1.41) [82].

The ventricular SAECG is most frequently used in patients recovering from myocardial infarction. Studies during the 1980s showed that late potentials are recorded much more frequently (in up to 93%) in patients recovering from myocardial infarction who develop sustained ventricular arrhythmias or sudden cardiac death. Although the presence of late potentials is not a highly specific or sensitive marker of sudden cardiac death, SAECG was considered a useful test, alone or in combination with other risk factors, for prediction of arrhythmic events in patients recovering from myocardial infarction because of its high (up to 97%) negative predictive value despite its very low (about 20%) positive predictive value [75,83].

The widespread use of thrombolysis/revascularization, beta-blockers and other advances in the treatment of myocardial infarction during the 1990s considerably decreased the rate of sudden cardiac death and sustained ventricular arrhythmias [84] and reduced the prevalence of late potentials following myocardial infarction [85]. Recent large studies on patients receiving modern treat-

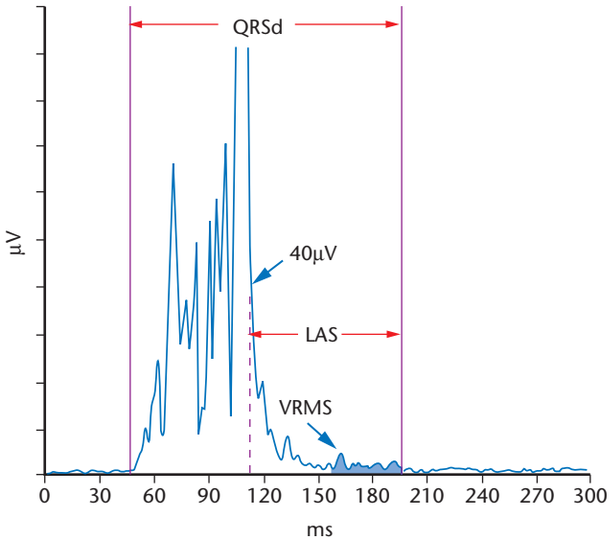

Figure 1.40 Schematic presentation of the three parameters that characterize the filtered QRS complex of the ventricular signal-averaged ECG. Note the low noise level of all three recordings.

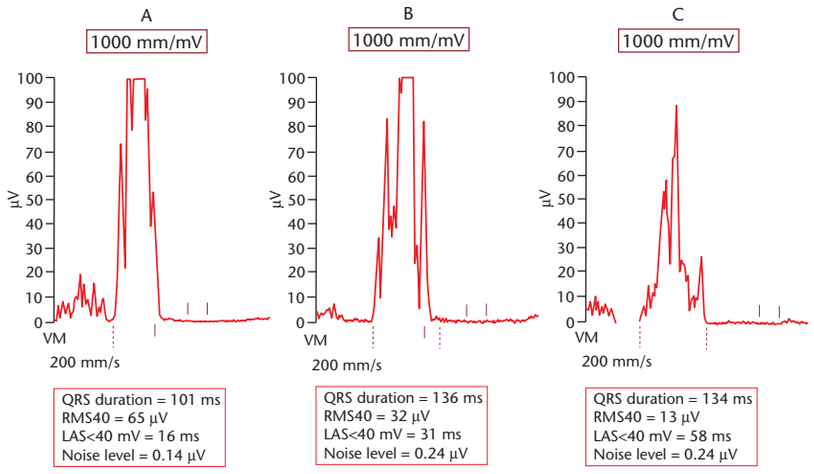

Figure 1.41 Examples of normal and abnormal ventricular signal-averaged ECG (SAECG). (A) Normal SAECG. (B) SAECG recorded in a 67-year-old man with mild heart failure and no history of arrhythmias. Only the filtered QRS duration is prolonged. (C) A clearly abnormal SAECG recorded in a man with severe heart failure. Note that all three parameters of the filtered QRS are abnormal.

ment after myocardial infarction demonstrated greatly reduced predictive power of SAECG for sudden cardiac death following myocardial infarction [86]. Nonetheless, a recently published substudy of the Multicenter Unsustained Tachycardia Trial (MUSTT) [87] demonstrated that in patients with ischaemic heart disease, left ventricular ejection fraction < 40% and non-sustained ventricular tachycardia, a filtered QRS duration > 114 ms was an independent predictor of cardiac and arrhythmic mortality. Because of its high negative predictive value (> 90%), SAECG is considered useful in the management of patients with syncope of unknown cause and ischaemic heart disease [75].

The value of SAECG in non-ischaemic cardiac diseases is less well investigated and established. Late potentials have been shown to independently predict adverse outcome in patients with non-ischaemic dilated cardiomyopathy in some studies [88] but not in others [89]. Although late potentials are more frequently recorded in patients with hypertrophic cardiomyopathy compared with healthy subjects, SAECG does not seem to have practical value for prediction of arrhythmic events in these patients [90]. Due to the localized character of the conduction abnormalities, SAECG can be useful as an additional diagnostic test in arrhythmogenic right ventricular cardiomyopathy [91].

In addition to time-domain analysis, other methods of analysis of the SAECG, such as spectrotemporal analysis [92,93], spectral turbulence analysis [94] and methods of high-resolution electrocardiography not based on temporal averaging (e.g. spatial averaging, which enables beat-to-beat analysis of late potentials [95]), have also been proposed but their clinical applicability is still unknown.

Atrial signal-averaged electrocardiography

Signal-averaged electrocardiography of the P wave (P-SAECG) was developed during the 1990s [96,97] as a result of growing awareness of the enormous clinical and socioeconomic significance of atrial fibrillation (AF) and hence of the need for simple and easily applicable methods for prediction of its occurrence or recurrence. Similarly to ventricular SAECG, the goal of P-SAECG is to detect and quantify intra-atrial conduction defects, one of the main factors for development of AF, which cannot simply be discerned from the shape and duration of the P wave on the standard ECG [98,99].

At present, most clinical studies have been performed using time-domain analysis of the P-SAECG. Similarly to ventricular SAECG, the filtered X, Y and Z leads are combined into a vector magnitude, and the latter is characterized by a set of parameters, such as the filtered P-wave duration, the integral of the P wave and the amplitude (RMS voltage) in different segments (e.g. the last 10, 20 or 30 ms) [96].

Several studies have demonstrated that the preoperatively assessed P-SAECG (mainly increased signal-averaged P-wave duration) independently predicts occurrence of AF following coronary artery bypass surgery [100–104]. P-SAECG has been shown to be useful for identifying patients at risk of transition from paroxysmal to sustained forms of AF [105], for prediction of AF recurrence after cardioversion [106,107], for prediction of paroxysmal AF in patients with congestive heart failure [108] and for assessment of antiarrhythmic drug efficacy for prophylaxis of paroxysmal AF [109].

A limited number of studies suggest that spectral analysis of the P-SAECG can provide additional information to the standard time-domain methods, but its clinical value is still unknown.

Microvolt T-wave alternans

Visible variations of the shape, amplitude or polarity of the T wave on an alternate-beat basis, described as T-wave alternans, have been recognized as a harbinger of ventricular arrhythmias in many clinical conditions, such as congenital long QT syndrome, myocardial ischaemia, electrolyte disturbance and toxic myocarditis [110–112]. In the 1980s, progress in computerized electrocardiography and signal processing led to the discovery, and routine clinical assessment, of microvolt (a few milliseconds) T-wave alternans (MTWA) induced by an increase in heart rate and invisible to the naked eye [113]. Subsequently, experimental studies demonstrated that MTWA is caused by non-uniform alterations (sequential shortening and lengthening) of action potential duration in different parts of the myocardium, which produce repolarization gradients that alternate in magnitude and direction on every other beat and thus create conditions for re-entry [114,115].

The methodology of measurement, the technical aspects and the interpretation of MTWA tests have recently been reviewed in detail (Fig. 1.42) [116]. Whilst early clinical studies used invasive atrial pacing in order to achieve the necessary increase in heart rate [117], currently MTWA is assessed using bicycle or treadmill exercise. Hohnloser *et al*. [118] demonstrated that the two methods were equivalent, both in terms of average heart rate at which MTWA becomes detectable and in terms of diagnostic yield.

During the last decade, a number of clinical studies have demonstrated a strong link between abnormal MTWA and arrhythmic events including sudden cardiac death in different cardiac patient populations [119,120]. Abnormal MTWA has been shown to strongly predict inducibility of ventricular tachycardia or ventricular fibrillation during electrophysiological study [121,122] and all-cause mortality [123] or arrhythmic events in patients recovering after myocardial infarction [124,125] and in those with dilated cardiomyopathy [126,127], Brugada's syndrome [128], non-ischaemic cardiomyopathy [129] or heart failure [130].

Three recent studies have demonstrated that MTWA testing can identify patients at high risk of arrhythmic death who might benefit from an implantable cardioverter-defibrillator (ICD) within the population of patients with left ventricular dysfunction after myocardial infarction (MADIT II type patients). In a meta-analysis of patients drawn from two previously published prospective studies on MTWA, Hohnloser *et al*. [131] reported a 15.6% rate of cardiac arrest or sudden cardiac death during a follow-up of 24 months in patients who tested positive or indeterminate (non-negative) for MTWA compared with no events in MTWA-negative patients ($P = 0.02$). Chow *et al*. [132] followed up similar patients for 18 months and reported an 11.8% rate of arrhythmic events (arrhythmic death, resuscitated cardiac arrest, or appropriate ICD discharge) among MTWA-positive patients compared with 2.0% among those who were MTWA negative (relative risk 6.0, $P = 0.035$). Bloomfield *et al*. [133] reported that the actuarial 2-year all-cause mortality rate of patients with abnormal (positive or indeterminate) MTWA was 17.8% compared with 3.2% of patients with negative MTWA (hazard ratio 4.8, $P = 0.02$). The mortality rate of patients with negative MTWA was only 3.8% (3.5% false-negative tests), which suggests that the test could be used for identifying MADIT II type patients who are at low arrhythmic risk and unlikely to benefit from an ICD.

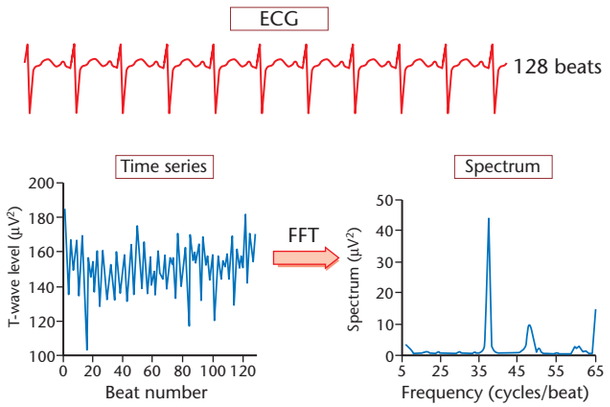

Figure 1.42 Principles of spectral analysis of microvolt T-wave alternans. The amplitudes of the T waves of 128 consecutive beats are measured and a time series consisting of these 128 amplitudes is constructed. The power spectrum of this time series is computed using fast Fourier transform (FFT) analysis. In the power spectrum obtained from recordings during bicycle exercise, peaks corresponding to frequencies of respiration, pedalling and alternans are shown. Microvolt T-wave alternans appears as a peak at half the beat frequency (0.5 cycles/beat). The amplitude of this peak is compared with the mean and standard deviation of the spectrum in a reference 'noise band'. Reprinted with permission from Cohen RJ. TWA and Laplacian imaging. In: Zipes DP, Jalife J (eds) *Cardiac Electrophysiology: From Cell to Bedside*, 2000. Philadelphia: WB Saunders, pp. 781–789.

Personal perspective

It is said by some that the 12-lead ECG could be reduced to a report and the trace itself omitted. For example, in many hospitals it is customary to receive nuclear scintigram reports and even radiography reports without copies of the images themselves. These experiences naturally frustrate most cardiologists, who would like to see the 'raw data' on which others have commented in order that they can make decisions relevant to the life and livelihood of their patients. Analysing the ECG or other images, especially as medical informatics and information technology improves, should not be a technical problem and the cardiologist should insist upon this. Examining the quality of the image, assessing the accuracy and confidence of the report, and assembling multiple images, technical information and patients' details are crucial to modern medicine.

Although electrocardiography is a well-established technique, the refinement of computer interpretation algorithms, improvements in recording technology and the development of completely new techniques (such as T-wave alternans, implantable ECG rhythm and ST-segment surveillance and logging, and very long-term wearable monitoring systems) will continue to evolve. High-resolution electrocardiography, for detecting early disease, discerning the effects of medications on the ECG and the prediction of electrical instability of the heart, will continue to develop. Web-based, ECG-related, patient-accessed systems will become more popular world-wide.

References

1 Bayés de Luna A. *Clinical Electrocardiography: A Textbook*, 2nd edn, 1999. New York: Futura.
2 Cranefield PF. *The Conduction of the Cardiac Impulse*, 1975. Mount Kisco, NY: Future.
3 Grant RP. *Clinical Electrocardiography: The Spatial Vector Approach*, 1957. New York: McGraw Hill.
4 McFarlane P, Veitch Lawrie TD (eds) *Comprehensive Electrocardiography*, 1989. Oxford: Pergamon Press.
5 Surawicz B (ed.). *Chou's Electrocardiography in Clinical Practice*, 5th edn, 1996. Philadelphia: WB Saunders.
6 Sodi D, Bisteni A, Medrano G. *Electrocardiografía y Vectorcardiografía Deductivas*, Vol. I, 1964. México DF: La Prensa Médica Mexicana.
7 Malik M, Camm AJ (eds) *Dynamic Electrocardiography*, 2004. Oxford: Blackwell Publishing.
8 Moss AJ. Long QT syndrome. *JAMA* 2003; **289**: 2041–2044.
9 Yap YG, Camm AJ. Drug induced QT prolongation and torsades de pointes. *Heart* 2003; **89**: 1363–1372.
10 Gaita F, Giustetto C, Bianchi F *et al*. Short QT syndrome: a familial cause of sudden death. *Circulation* 2003; **108**: 965–970.
11 Durrer D, Van Dam R, Freud G, Janse M, Meijler F, Arzbaecher R. Total excitation of the isolated human heart. *Circulation* 1970; **41**: 899–912.
12 Bayés de Luna A, Fort de Ribot R, Trilla E *et al*. Electrocardiographic and vectrocardiographic study of interatrial conduction disturbances with left atrial retrograde activation. *J Electrocardiol* 1985; **18**: 1–13.
13 Bayés de Luna A, Cladellas M, Oter R *et al*. Interatrial conduction block and retrograde activation of the left atrium and paroxysmal supraventricular tachyarrhythmias. *Eur Heart J* 1988; **9**: 1112–1118.
14 Wagner GS (ed.) *Marriot's Practical Electrocardiography*, 10th edn, 2001. Philadelphia: Lippincott Williams & Wilkins.
15 Horan LG, Flowers NC. ECG and VCG. In: Braunwald E (ed.). *Heart Disease*, 1980. Philadelphia: WB Saunders.
16 Bayés de Luna A, Carrio I, Subirana MT *et al*. Electrophysiological mechanism of the $S_I S_{II} S_{III}$ electrocardiographic morphology. *J Electrocardiol* 1987; **20**: 38.
17 Bayés de Luna A, Serra Genís C, Guix M. Septal fibrosis as determinant of Q waves in patients with aortic valve disease. *Eur Heart J* 1983; **4** (suppl. E): 86.
18 Piccolo E, Raviele A, Delise P *et al*. The role of left ventricular conduction in the electrogenesis of left ventricular hypertrophy. An electrophysiologic study in man. *Circulation* 1979; **59**: 1044–1055.
19 Rosenbaum MB, Elizari MV, Lazzari JO. *Los Hemibloqueos*, 1968. Buenos Aires: Ed. Paidos.
20 Wolff L, Parkinson J, White DD. Bundle branch block with short PR interval in healthy young people prone to paroxysmal tachycardia. *Am Heart J* 1930; **5**: 685.
21 Lown B, Ganong WF, Levine SA. The syndrome of short PR interval, normal QRS complex and paroxysmal rapid heart beat. *Circulation* 1957; **5**: 693–706.
22 Sternick EB, Timmermans C, Sosa E *et al*. The electrocardiogram during sinus rhythm and tachycardia in patients with Mahaim fibers. *J Am Coll Cardiol* 2004; **44**: 1626–1635.
23 Montoya PT, Brugada P, Smeets J *et al*. Ventricular fibrillation in the Wolff–Parkinson–White syndrome. *Eur Heart J* 1991; **12**: 144–150.
24 Wellens HJ, Atie J, Smeets JL, Cruz FE, Gorgels AP, Brugada P. The ECG in patients with multiple accessory pathways. *J Am Coll Cardiol* 1990; **16**: 745–751.
25 Milstein S, Sharma AD, Guiraudon GM, Klein GJ. An algorithm for the electrocardiographic localization of

accessory pathways in the Wolff–Parkinson–White syndrome. *Pacing Clin Electrophysiol* 1987; **10**: 555–563.
26 Hathaway WR, Peterson ED, Wagner GS *et al*. Prognostic significance of the initial electrocardiogram in patients with acute myocardial infarction. GUSTO-I Investigators. Global Utilization of Streptokinase and t-PA for Occluded Coronary Arteries. *JAMA* 1998; **279**: 38–91.
27 Wellens HJ, Gorgels A, Doevendans PA. *The ECG in Acute Myocardial Infarction and Unstable Angina*, 2003. Boston: Kluwer Academic Publishers.
28 Engelen DJ, Gorgels AP, Cheriex EC *et al*. Value of electrocardiogram in localizing the occlusion site in the left anterior descending coronary artery in acute anterior myocardial infarction. *J Am Coll Cardiol* 1999; **34**: 389–395.
29 Sclarowsky S. *Electrocardiography of Acute Myocardial Ischemia*, 1999. London: Martin Dunitz.
30 Fiol M, Cygankiewicz I, Guindo J *et al*. Evolving myocardial infarction with ST elevation: ups and downs of ST in different leads identifies the culprit artery and location of the occlusion. *Ann Noninvasive Electrocardiol* 2004; **9**: 180–186.
31 Fiol M, Cygankiewicz I, Bayés Genis A *et al*. The value of ECG algorithm based on 'ups and downs' of ST in assessment of a culprit artery in evolving inferior myocardial infarction. *Am J Cardiol* 2004; **94**: 709–714.
32 Fiol M, Carillo A, Cygankiewicz I *et al*. New criteria based on ST changes in 12 leads surface ECG to detect proximal vs. distal right coronary artery occlusion in case of an acute inferoposterior myocardial infarction. *Ann Noninvasive Electrocardiol* 2004; **9**: 383–389.
33 Sadanandan S, Hochman S, Kolodziej A *et al*. Clinical and angiographic characteristics of patients with combined anterior and inferior ST segment elevation in the initial ECG during acute myocardial infarction. *Am Heart J* 2003; **146**: 653–661.
34 Yamaji H, Iwasaki K, Kusachi S *et al*. Prediction of acute left main coronary artery obstruction by 12 lead electrocardiography. ST segment elevation in lead VR with less ST segment elevation in lead V1. *J Am Coll Cardiol* 2001; **48**: 1348–1354.
35 Nikus KC, Escola MJ, Virtanen VK *et al*. ST depression with negative T waves in leads V4–V5: a marker of a severe coronary artery disease in non-ST elevation acute coronary syndrome: a prospective study of angina at rest with troponin, clinical, electrocardiographic, and angiographic correlation. *Ann Noninvasive Electrocardiol* 2004; **9**: 207–214.
36 Bayés de Luna A, Carreras F, Cladellas M, Oca F, Sagues F, Garcia Moll M. Holter ECG study of the electrocardiographic phenomena in Prinzmetal angina attacks with emphasis on the study of ventricular arrhythmias. *J Electrocardiol* 1985; **18**: 267–275.
37 European Society of Cardiology/American College of Cardiology. Myocardial infarction redefined: a consensus document of the Joint European Society of Cardiology/American College of Cardiology Committee for the redefinition of myocardial infarction. *Eur Heart J* 2000; **21**: 1502–1513.
38 Wagner GS, Bahit MC, Criger D *et al*. Toward a new definition of acute myocardial infarction for the 21st century: status of the ESC/ACC consensus conference. *J Electrocardiol* 2000; **33** (suppl.): 57–59.
39 Phibbs B, Marcus F, Marriott HJ, Moss A, Spodick DH. Q-wave versus non-Q wave myocardial infarction: a meaningless distinction. *J Am Coll Cardiol* 1999; **33**: 576–582.
40 Moon JCC, Perez de Arenaza P, Elkington AG *et al*. The pathologic basis of Q wave and non-Q wave myocardial infarction. A cardiovascular magnetic resonance study. *J Am Coll Cardiol* 2004; **44**: 554–560.
41 Myers GB, Klein HA, Stofer BE. Correlation of ECG findings in anteroseptal infarction. *Am Heart J* 1948; **36**: 535.
42 Bogaty P, Boyer L, Rousseau L, Arsenault M. Is anteroseptal myocardial infarction an appropriate term? *Am J Med* 2002; **113**: 37–41.
43 Selvanayagam JB, Kardos A, Nicolson D *et al*. Anteroseptal and apical myocardial infarction: a controversy addressed using delayed enhancement cardiovascular magnetic resonance imaging. *J Cardiovasc Magn Reson* 2004; **6**: 653–661.
44 Cerqueira MD, Weissman NJ, Disizian V *et al*. Standarized myocardial segmentation and nomenclature for tomographic imaging of the heart. A statement for healthcare professionals from the Cardiac Imaging Committee of the Council on Clinical Cardiology of the American Heart Association. *Circulation* 2002; **105**: 539–542.
45 Bayés de Luna A, Cino J, Pujadas S *et al*. Concordance of electrocardiographic patterns and healed myocardial infarction location detected by cardiovascular magnetic resonance. *Am J Cardiol* 2006 (in press).
46 Cino JM, Pujadas S, Carreras F *et al*. Utility of contrast-enhanced cardiovascular magnetic resonance (CE-CMR) to assess the sensitivity and specificity of different ECG patterns to locate Q-wave myocardial infarction. *J Cardiovasc Magn Reson* 2005 (in press).
47 Selvester RH, Wagner GS, Hindman NB. The Selvester QRS scoring system for estimating myocardial infarction size: the development and application of the system. *Arch Intern Med* 1985; **145**: 1877–1881.
48 Engblom H, Wagner GS, Sester RM *et al*. Quantitative clinical assessment of chronic anterior myocardial infarction with delayed enhancement magnetic resonance imaging and QRS scoring. *Am Heart J* 2003; **146**: 359–366.
49 Marcassa C, Galli M, Paino A, Campini R, Giubbini R, Giannuzzi P. Electrocardiographic evolution after Q wave anterior myocardial infarction: correlations between QRS score and changes in left ventricular perfusion and function. *J Nucl Cardiol* 2001; **8**: 561–567.
50 Sgarbossa EB, Pinski SL, Barbagelata A *et al*. Electrocardiographic diagnosis of evolving acute myocardial infarction in the presence of left bundle-

branch block. GUSTO-1 (Global Utilization of Streptokinase and Tissue Plasminogen Activator for Occluded Coronary Arteries) Investigators. *N Engl J Med* 1996; **334**: 481.
51 Wackers F, Lie KL, David G, Durrer D, Wellens HJJ. Assessment of the value of the ECG signs for myocardial infarction in left bundle branch block by thallium. *Am J Cardiol* 1978; **41**: 428.
52 Sgarbossa E, Pinski S, Gates K, Wagner G. Early ECG diagnosis of acute myocardial infarction in the presence of ventricular paced rhythm. *Am J Cardiol* 1996; **77**: 423–424.
53 Akurisu S, Sato H, Kawagoe T *et al*. Left ventricular dysfunction with ST elevation: a novel cardiac syndrome mimicking acute myocardial infarction. *Am Heart J* 2002; **143**: 448–455.
54 Breithardt G, Cain ME, El-Sherif N *et al*. Standards for analysis of ventricular late potentials using high resolution or signal-averaged electrocardiography. A statement by a Task Force Committee between the European Society of Cardiology, the American Heart Association and the American College of Cardiology. *Eur Heart J* 1991; **12**: 473–480.
55 Kulakowski P. Ventricular signal averaged electrocardiography. In: Malik M (ed.). *Risk of Arrhythmia and Sudden Death*, 2001. London: BMJ Books, pp. 167–179.
56 Michelucci A, Padeletti L, Colella A *et al*. Signal averaged P wave. In: Malik M (ed.). *Risk of Arrhythmia and Sudden Death*, 2001. London: BMJ Books, pp. 180–186.
57 Verrier RL, Nearing BD, Stone PH. Optimizing ambulatory ECG monitoring of T-wave alternans for arrhythmia risk assessment. *Card Electrophysiol Rev* 2002; **6**: 329–333.
58 Surawicz B, Knilans TK. Misplacement of leads and electrocardiographic artifacts. In: Surawicz B, Knilans TK (eds). *Chou's Electrocardiography in Clinical Practice*, 5th edn, 1996. Philadelphia: WB Saunders, pp. 569–582.
59 Macfarlane PW, Coleman EN. Resting 12-lead ECG electrode placement and associated problems. Available at http://www.scst.org.uk/coleman/resting.htm
60 Wagner GS. Correct and incorrect lead placement. In: Wagner GS (ed.). *Marriot's Practical Electrocardiography*, 10th edn, 2001. Philadelphia: Lippincott Williams & Wilkins, pp. 33–34.
61 Haisty WK, Pahlm O, Edenbrandt L, Newman K. Recognition of electrocardiographic electrode misplacements involving the ground (right leg) electrode. *Am J Cardiol* 1993; **71**: 1490–1495.
62 Rauraharju PM, Park L, Rautaharju FS, Crow R. A standardized procedure for locating and documenting ECG chest electrode positions. Consideration of the effect of breast tissue on ECG amplitudes in women. *J Electrocardiol* 1998; **31**: 17–29.
63 August T, Mazzeleni A, Wolff L. Positional and respiratory changes in precordial lead patterns simulating acute myocardial infarction. *Am Heart J* 1958; **55**: 706–714.
64 Zema MJ, Luminais SK, Chiaramida S *et al*. Electrocardiographic poor R wave progression III: the normal variant. *J Electrocardiol* 1980; **13**: 135–142.
65 Herman MV, Ingram DA, Levy JA *et al*. Variability of electrocardiographic precordial lead placement: a method to improve accuracy and reliability. *Clin Cardiol* 1991; **14**: 469–476.
66 Kerwin A J, McLean R, Tegelaar H. A method for the accurate placement of chest electrodes in the taking of serial electrocardiographic tracings. *Can Med Assoc J* 1960; **82**: 258–261.
67 Wenger W, Kligfield P. Variability of precordial electrode placement during routine electrocardiography. *J Electrocardiol* 1996; **29**: 179–184.
68 Society for Cardiological Science and Technology. Clinical Guidelines by Consensus. Number 1. Recording a standard 12-lead electrocardiogram. Available at http://www.scst.org.uk/docs/Consensus%20guidelines%20for%20recording%20a%2012%20lead%20ECG.pdf. Accessed on 16 June 2005.
69 Colaco R, Reay P, Beckett C, Aitchison TC, Macfarlane PW. False positive ECG reports of anterior myocardial infarction in women. *J Electrocardiol* 2000; **33**: 239–244.
70 Macfarlane PW, Colaco R, Stevens K, Reay P, Beckett C, Aitchison T. Precordial electrode placement in women. *Neth Heart J* 2003; **11**: 118–122.
71 Pahlm O, Halsty WK, Edenbrandt L *et al*. Evaluation of change in standard electrocardiographic QRS waveforms recorded from activity-compatible proximal limb lead positions. *Am J Cardiol* 1992; **69**: 253–257.
72 Pipberger HV, Arzbaecher RC, Berson AS *et al*. Report of the Committee on Electrocardiography of the American Heart Association. Recommendations for standardization of leads and of specifications for instruments in electrocardiography and vectorcardiography. *Circulation* 1975; **52**: 11–31.
73 Mason RE, Likar I. A new system of multi-lead exercise electrocardiography. *Am Heart J* 1966; **71**: 196–205.
74 Papaouchado M, Walker PR, James MA, Clarke LM. Fundamental differences between the standard 12-lead electrocardiograph and the modified (Mason–Likar) exercise lead system. *Eur Heart J* 1987; **8**: 725–733.
75 Berbari EJ. High-resolution electrocardiography. In: Zipes DP, Jalife J (eds). *Cardiac Electrophysiology: From Cell to Bedside*, 4th edn, 2004. Philadelphia: WB Saunders, Elsevier, pp. 793–802.
76 Breithardt G, Cain ME, El-Sherif N *et al*. Standards for analysis of ventricular late potentials using high resolution electrocardiography. A statement by a Task Force Committee between the European Society of Cardiology, the American Heart Association and the American College of Cardiology. *J Am Coll Cardiol* 1991; **17**: 999–1006.
77 Lander P, Berbari EJ. Principles and signal-processing techniques of the high-resolution electrocardiogram. *Prog Cardiovasc Dis* 1992; **35**: 169–188.
78 Boineau JP, Cox JL. Slow ventricular activation in acute myocardial infarction. A source of re-entrant premature ventricular contraction. *Circulation* 1973; **48**: 702–713.
79 El-Sherif N. Electrophysiologic basis of ventricular late potentials. *Prog Cardiovasc Dis* 1993; **35**: 417–427.

80 Gardner PI, Ursell PC, Fenoglio JJ, Wit AL. Electrophysiologic and anatomic basis for fractionated electrograms recorded from healed myocardial infarcts. *Circulation* 1985; **72**: 596–611.

81 ACC Expert Consensus Document. Signal-averaged electrocardiography. *J Am Coll Cardiol* 1996; **27**: 238–249.

82 Savard P, Rouleau JL, Ferguson J *et al*. Risk stratification after myocardial infarction using signal-averaged electrocardiographic criteria adjusted for sex, age and myocardial infarction. *Circulation* 1997; **96**: 202–213.

83 Kulakowski P. Clinical utility of signal-averaged electrocardiography. *Card Electrophysiol Rev* 1997; **3**: 321–324.

84 Huikuri HV, Tapanainen JM, Lindgren K *et al*. Prediction of sudden cardiac death after myocardial infarction in the beta-blocking era. *J Am Coll Cardiol* 2003; **42**: 652–658.

85 Beauregard LA, Waxman HL, Volosin R, Volosin KJ, Kurnik PB. Signal averaged ECG prior to and serially after thrombolytic therapy for acute myocardial infarction. *Pacing Clin Electrophysiol* 1996; **19**: 883–889.

86 Bauer A, Guzik P, Barthel P *et al*. Reduced prognostic power of ventricular late potentials in post-infarction patients of the reperfusion era. *Eur Heart J* 2005; **26**: 755–761.

87 Gomes JA, Cain ME, Buxton AE *et al*. Prediction of long-term outcomes by signal-averaged electrocardiography in patients with unsustained ventricular tachycardia, coronary artery disease, and left ventricular dysfunction. *Circulation* 2001; **104**: 436–441.

88 Mancini DM, Wong KL, Simson MB. Prognostic value of an abnormal signal-averaged electrocardiogram in patients with non-ischemic congestive cardiomyopathy. *Circulation* 1993; **87**: 1083–1092.

89 Middlekauff HR, Stevenson WG, Woo MA *et al*. Comparison of frequency of late potentials in idiopathic dilated cardiomyopathy and ischemic cardiomyopathy with advanced congestive heart failure and their usefulness in predicting sudden death. *Am J Cardiol* 1990; **66**: 1113–1117.

90 Fauchier J-P, Fauchier L, Babuty D, Cosnay P. Time-domain signal-averaged electrocardiogram in nonischemic ventricular tachycardia. *Pacing Clin Electrophysiol* 1996; **19**: 231–244.

91 Hamid MS, Norman M, Quraishi A *et al*. Prospective evaluation of relatives for familial arrhythmogenic right ventricular cardiomyopathy/dysplasia reveals a need to broaden diagnostic criteria. *J Am Coll Cardiol* 2002; **40**: 1445–1450.

92 Zbilut JP, Buckingham TA. Overview of frequency–time (spectro-temporal) analysis of signal-averaged electrocardiograms. *Prog Cardiovasc Dis* 1993; **35**: 429–434.

93 Cain ME, Ambos HD, Lindsay BD, Arthur RM. Contributions of frequency analysis to the identification of the spectral, temporal, and spatial features in signal-averaged electrograms that distinguish patients prone to sustained ventricular arrhythmias. *Prog Cardiovasc Dis* 1992; **35**: 189–212.

94 Copie X, Hnatkova K, Staunton A, Camm AJ, Malik M. Spectral turbulence versus time-domain analysis of signal-averaged ECG used for the prediction of different arrhythmic events in survivors of acute myocardial infarction. *J Cardiovasc Electrophysiol* 1996; **7**: 583–593.

95 El-Sherif N, Mehra R, Restivo M. Beat-to-beat high resolution electrocardiogram: technical and clinical aspects. *Prog Cardiovasc Dis* 1993; **35**: 407–415.

96 Stafford PJ, Turner I, Vincent R. Quantitative analysis of signal-averaged P waves in idiopathic paroxysmal atrial fibrillation. *Am J Cardiol* 1991; **68**: 751–755.

97 Guidera SA, Steinberg JS. The signal-averaged P wave duration: a rapid non-invasive marker of risk for atrial fibrillation. *J Am Coll Cardiol* 1993; **21**: 1645–1651.

98 Jordaens L, Tavernier R, Gorgov N *et al*. Signal-averaged P wave: predictor of atrial fibrillation. *J Cardiovasc Electrophysiol* 1998; **9** (suppl. 8): S30–S34.

99 Darbar D, Jahangir A, Hammill SC, Gersh BJ. P wave signal-averaged electrocardiography to identify risk for atrial fibrillation. *Pacing Clin Electrophysiol* 2002; **25**: 1447–1453.

100 Stafford PJ, Kolvekar S, Cooper J *et al*. Signal averaged P wave compared with standard electrocardiography or echocardiography for prediction of atrial fibrillation after coronary bypass grafting. *Heart* 1997; **77**: 417–422.

101 Steinberg JS, Zelenkofske S, Wong S-C, Gelernt M, Sciacca R, Menchavez E. Value of the P-wave signal-averaged ECG for predicting atrial fibrillation after cardiac surgery. *Circulation* 1993; **88**: 2618–2622.

102 Klein M, Evans SJ, Blumberg S, Cataldo L, Bodeheimer MM. Use of P-wave-triggered, P-wave-signal-averaged electrocardiogram to predict atrial fibrillation after coronary bypass surgery. *Am Heart J* 1995; **129**: 895–901.

103 Zaman AG, Archbold RA, Helft G *et al*. Atrial fibrillation after coronary artery bypass surgery: a model for preoperative risk stratification. *Circulation* 2000; **101**: 1403–1408.

104 Yi Gang, Hnatkova K, Mandal K, Ghuran A, Malik M. Preoperative electrocardiographic risk assessment of atrial fibrillation after coronary artery bypass grafting. *J Cardiovasc Electrophysiol* 2004; **15**: 1379–1386.

105 Abe Y, Fukunami M, Yamada T *et al*. Prediction of transition to chronic atrial fibrillation in patients with paroxysmal atrial fibrillation by signal-averaged electrocardiography. A prospective study. *Circulation* 1997; **96**: 2612–2616.

106 Raitt MH, Thurman M, Ingram KD. P wave duration predicts the risk of early recurrence of atrial fibrillation after cardioversion. *J Am Coll Cardiol* 1999; **33**: 143A.

107 Opolski G, Scislo P, Stanislawska J, Gorecki A, Steckiewicz R, Torbicki A. Detection of patients at risk for recurrence of atrial fibrillation after successful electrical cardioversion by signal-averaged P-wave. *Int J Cardiol* 1997; **602**: 181–185.

108 Yamada T, Fukunami M, Shimonagat T et al. Prediction of paroxysmal atrial fibrillation in patients with congestive heart failure: a prospective study. *J Am Coll Cardiol* 2000; **35**: 405–413.

109 Banasiak W, Telichowski A, Anker SD *et al*. Effects of amiodarone on the P-wave triggered signal-averaged

electrocardiogram in patients with paroxysmal atrial fibrillation and coronary artery disease. *Am J Cardiol* 1999; **83**: 112–114.

110 Hering HE. Das Wesen des Herzalternans. *Muench Med Wochenschr* 1908; **4**: 1417–1421.

111 Surawicz B, Fisch C. Cardiac alternans: diverse mechanisms and clinical manifestations. *J Am Coll Cardiol* 1992; **20**: 483–499.

112 Lux RL, Brockmeier K. Macro T wave alternans. In: Malik M, Camm AJ (eds). *Dynamic Electrocardiography*, 2004. New York: Blackwell Publishing, Futura, pp. 433–438.

113 Adam DR, Powell AO, Gordon H, Cohen RJ. Ventricular fibrillation and fluctuations in the magnitude of the repolarization vector. *IEEE Comp Cardiol* 1982; 241–244.

114 Pastore JM, Girouard SD, Laurita KR *et al*. Mechanism linking T-wave alternans to the genesis of cardiac fibrillation. *Circulation* 1999; **99**: 1385–1394.

115 Pastore JM, Rosenbaum DS. Role of structural barriers in the mechanism of alternans-induced reentry. *Circ Res* 2000; **87**: 1157–1163.

116 Bloomfield DM, Hohnloser SH, Cohen RJ. Interpretation and classification of microvolt T wave alternans tests. *J Cardiovasc Electrophysiol* 2002; **13**: 502–512.

117 Rosenbaum DS, Jackson LE, Smith JM *et al*. Electrical alternans and vulnerability to ventricular arrhythmias. *N Engl J Med* 1994; **330**: 235–241.

118 Hohnloser SH, Klingenheben T, Zabel M *et al*. T wave alternans during exercise and atrial pacing in humans. *J Cardiovasc Electrophysiol* 1997; **8**: 987–993.

119 Armoundas AA, Tomaselli GF, Esperer HD. Pathophysiological basis and clinical application of T-wave alternans. *J Am Coll Cardiol* 2002; **40**: 207–217.

120 Hohnsloser SH. T-wave alternans. In: Zipes DP, Jalife J (eds). *Cardiac Electrophysiology: From Cell to Bedside*, 4th edn, 2004. Philadelphia: WB Saunders, Elsevier, pp. 839–847.

121 Gold MR, Bloomfield DM, Anderson KP *et al*. A comparison of T wave alternans, signal-averaged electrocardiography and programmed ventricular stimulation for arrhythmia risk stratification. *J Am Coll Cardiol* 2000; **36**: 2247–2253.

122 Estes NA III, Michaud G, Zipes DP *et al*. Electrical alternans during rest and exercise as predictors of vulnerability to ventricular arrhythmias. *Am J Cardiol* 1997; **80**: 1314–1318.

123 Tapanainen JM, Still AM, Airaksinen KEJ, Huikuri HV. Prognostic significance of risk stratifiers of mortality, including T wave alternans, after acute myocardial infarction: results of a prospective follow-up study. *J Cardiovasc Electrophysiol* 2001; **12**: 645–652.

124 Kitamura H, Ohnishi Y, Okajima K *et al*. Onset heart rate of microvolt-level T-wave alternans provides clinical and prognostic value in nonischemic dilated cardiomyopathy. *J Am Coll Cardiol* 2002; **39**: 295–300.

125 Ikeda T, Saito H, Tanno K *et al*. T-wave alternans as a predictor for sudden cardiac death after myocardial infarction. *Am J Cardiol* 2002; **89**: 79–82.

126 Adachi K, Ohnishi Y, Shima T *et al*. Determinant of microvolt T-wave alternans in patients with dilated cardiomyopathy. *J Am Coll Cardiol* 1999; **34**: 374–380.

127 Hohnloser SH, Klingenheben T, Bloomfield D *et al*. Usefulness of microvolt T wave alternans for prediction of ventricular tachyarrhythmic events in patients with dilated cardiomyopathy: results from a prospective observational study. *J Am Coll Cardiol* 2003; **41**: 2220–2224.

128 Ikeda T, Sakurada H, Sakabe K *et al*. Assessment of non-invasive markers in identifying patients at risk in the Brugada syndrome: insight into risk stratification. *J Am Coll Cardiol* 2001; **37**: 1628–1634.

129 Hennersdorf MG, Perings C, Niebch V, Vester EG, Strauer BE. T wave alternans as a risk predictor in patients with cardiomyopathy and mild-to-moderate heart failure. *Pacing Clin Electrophysiol* 2000; **23**: 1386–1391.

130 Klingenheben T, Zabel M, D'Agostino RB, Cohen RJ, Hohnloser SH. Predictive value of T-wave alternans for arrhythmic events in patients with congestive heart failure (letter). *Lancet* 2000; **356**: 651–652.

131 Hohnloser SH, Ikeda T, Bloomfield DM, Dabbous OH, Cohen RJ. T-wave alternans negative coronary patients with low ejection and benefit from defibrillator implantation. *Lancet* 2003; **362**: 125–126.

132 Chow T, Schloss E, Waller T *et al*. Microvolt T-wave alternans identifies MADIT II type patients at low risk of ventricular tachyarrhythmic events (abstract). *Circulation* 2003; **108**: IV-323.

133 Bloomfield DM, Steinman RC, Namerow PB *et al*. Microvolt T-wave alternans distinguishes between patients likely and patients not likely to benefit from implanted cardiac defibrillator therapy: a solution to the Multicenter Automatic Defibrillator Implantation Trial (MADIT) II conundrum. *Circulation* 2004; **110**: 1885–1889.